9-10-2015

Utilization Of Antibody-Conjugated Gold Nanoparticles, Dynamic Light Scattering And Sers In Influenza Virus Detection

Yen Hoang Lai
Illinois State University, laihoangyen@gmail.com

UTILIZATION OF ANTIBODY-CONJUGATED GOLD NANOPARTICLES, DYNAMIC LIGHT SCATTERING AND SERS IN INFLUENZA VIRUS DETECTION

Yen H. Lai

78 Pages

Influenza A H3N2, H1N1, and influenza B viruses primarily cause winter illness in humans, leading to significant morbidity and mortality in the population of the very young, the elderly, and people with chronic disease. In addition to the regular seasonal epidemics of influenza, influenza pandemics associated with the emergence of new influenza A strains are threatening due to high levels of mortality, social disruption, and economic losses. These novel strains are not affected by the human immunity developed to older strains of influenza, therefore can spread readily and infect a vast number of people. The most recent flu pandemic outbreak was in 2009, in which pandemic swine influenza A H1N1 was transmitted. Thus, an initiative to prevent human infections with new strains of influenza A virus with pandemic potential has been supported by the government and become a focus of many laboratories. The first step in any preventative measures is early detection. Therefore, it is essential to develop a detection platform that is capable of simultaneous multiplexing and exploitable for point-of-care (POC) analysis.

Virus culture, nucleic acid testing, and immunoassays are primary detection approaches to confirm acute human influenza virus infection. Nucleic acid testing has great sensitivity and specificity to subtype influenza strains, and high capacity for multiplexed detection. However, it is time and labor intensive, and expensive. Virus isolation is slow, costly, and not feasible for routine diagnostic testing. Immunoassays, in contrast, are known for availability, low-cost, accuracy, and versatility, and therefore have become a centerpiece in diagnostics. Among a number of analytical detection techniques developed for immunoassays, SERS (surface enhanced Raman spectroscopy) biosensing utilizing antibody-conjugated gold nanoparticles (Ab-AuNPs) is a promising virus detection technique providing high sensitivity (down to single molecule detection) and multiplexing (distinction of different strains of a single virus type).

Herein a simple, rapid, sensitive AuNP-based immunoassay was developed to quantitatively detect influenza A virus, utilizing dynamic light scattering (DLS) and surface enhanced Raman spectroscopy (SERS). The assay platform was established based on the principle of homogeneous format. Antigen-specific antibodies (Abs) were attached to the surface of gold nanoparticles (AuNPs), rendering the biospecificity for the detection. AuNPs serve as a signal generator or label. A biological sample containing targeted analytes was mixed with Ab-conjugated AuNPs (or AuNP probes); aggregation of nanoparticle was induced in the presence of the analyte(s). The antibody molecules on the particle surface recognized and bound to the analyte via the key-lock like mechanism, cross-linking AuNPs together to form aggregates. The quantification of antigen became the matter of detecting aggregation. The reaction happened in a timely fashion, oftentimes in a few minutes owing to the fast solution phase kinetics. No washing was

required; therefore, time and labor were remarkably saved relative to heterogeneous assays. When utilizing this platform, alteration of different antigen-specific antibodies can perform detection of different antigen analytes individually (singleplexing). The combination of multiple types of AuNP probes in one assay allows simultaneously multiplexed detection.

In order to ensure the robustness of the assay, optimization for each stage of the platform design was thoroughly studied. The optimal conditions for maintaining the stability of the gold nanoparticles coated with monoclonal antibodies (mAbs) were investigated by varying pH, conjugation chemistry, mAbs concentrations, and blocking reagents. DLS is exploited to monitor the conjugation of the antibodies on AuNPs and verify the aggregate formation of the antigen-induced AuNP probes based on hydrodynamic diameter measurements. The DLS-based immunoassay has been demonstrated as an excellent rapid screening method to evaluate the specificity and affinity of antibody-antigen binding. Comparing to a conventional method for antibody screening (i.e. ELISA), a DLS assay requires only 30 min while it takes 24 h to perform an ELISA.

To address the urgent need for multiplexed detection, we have slightly modified the DLS assay to develop a SERS-based homogeneous immunoassay. Namely, Raman reporters and antibody were co-immobilized on the AuNPs to construct ERLs (extrinsic Raman labels). Raman reporters provide distinctive and amplified signal for detection. In order to detect multiple analytes, multiple types of ERLs were separately prepared; each type was a unique combination of one antigen-specific antibody and one Raman reporter. The ERLs were then mixed together and added to the sample. Aggregation was induced

upon the introduction of the antigen to the suspension of ERLs on the order of minutes. ERLs of the same type were cross-linked via the antigen specific to the antibody conjugated to the very type of ERLs. The nonspecific ERLs remained unreacted if their antigens were not present in the sample. Once aggregation occurred, the SERS signals provided by the Raman reporters on the reacted ERLs were turned on. AuNPs in the aggregating state were in proximity to each other and created small gaps between them. Raman reporters once trapped in those gaps generated signal for detection. In theory, SERS analysis can be performed in solution but in reality poor plasmonic coupling between antibody-modified AuNP limits the SERS enhancement. However, dehydration of the aggregates reduces interparticle spacing to yield higher SERS signals. Therefore, separation of aggregated ERLs on a well-defined nanoporous membrane was applied to intensify the signal. The conditions for optimal filtration process have been investigated. Preliminary data have shown progress made toward a fully developed configuration for a portable multiplexed, sensitive, and rapid POC detection platform.

KEYWORDS: Antibody-Antigen Binding Properties SERS, Antibody Conjugation, Direct Adsorption, DLS, ERLs, Gold Nanoparticle Probes, Homogeneous Immunoassay, Influenza Virus Detection, Nanoparticle Aggregates, Raman Reporters

UTILIZATION OF ANTIBODY-CONJUGATED GOLD NANOPARTICLES, DYNAMIC LIGHT SCATTERING AND SERS IN INFLUENZA VIRUS DETECTION

YEN H. LAI

A Thesis Submitted in Partial
Fulfillment of the Requirements
for the Degree of

MASTER OF SCIENCE

Department of Chemistry

ILLINOIS STATE UNIVERSITY

2015

UTILIZATION OF ANTIBODY-CONJUGATED GOLD NANOPARTICLES, DYNAMIC LIGHT SCATTERING AND SERS IN INFLUENZA VIRUS DETECTION

YEN H. LAI

COMMITTEE MEMBERS:

Jeremy Driskell, Chair

Jun-Hyun Kim

Jon Friesen

ACKNOWLEDGMENTS

The writer wishes to give special thanks to Dr. Jeremy Driskell, for being the most understanding, caring, and supportive research advisor.

I wish to thank Dr. Cedeno and his wife, for their belief in me. Without their support, this amazing journey could have never begun.

I wish to thank my best cousin, Chau, for the sweet companionship.

I wish to thank my family for their love and nurture.

I wish to thank my friends at the department for all the moments we have shared at the Department of Chemistry.

I also wish to thank Dr. Jun-Hyun Kim for his guidance and support throughout my graduate studies.

Finally, I wish to express my gratitude to the faculty, staff, and students of the Department of Chemistry and Illinois State University for providing such a great learning environment.

Y. H. L.

CONTENTS

FIGURES

CHAPTER I

INTRODUCTION

Influenza A Virus- Impact on Society

Influenza viruses cause a contagious respiratory illness, commonly called flu. Even though most people infected with flu have mild illness, some high-risk groups might have severe flu complications, which may result in hospitalization and death. Influenza virus outbreaks occur annually from October through May with flu activity peaks between December and February, but the severity of outbreaks differs. Despite a long history of defending humans against influenza A via a number of preventive strategies, influenza epidemics still account for significant morbidity and mortality every year with the average of 9,187 deaths and 128,710 hospitalizations. [1] The estimation of the total economic burden of seasonal influenza and influenza complication in the US is $87.1 billion. [1a] In addition to seasonal epidemics, influenza pandemics with the emergence of new influenza A strains are potentially threatening. These novel strains, evolved by a dynamic combination of mutations and frequent re-assortment (known as antigen shift) [1b, 2], are not affected by the human immunity. Furthermore, the diverse genomic evolution may result in virus infection to multiple animal hosts. This incident may increase the frequencies of transmission from animals to humans and among humans, therefore can readily spread and infect a vast number of people. The most recent pandemic outbreak occurred worldwide in 2009 with an unprecedented speed, in which

swine-origin influenza viruses A/H1N1 (S-OIVs, re-assortment of swine H1N1, avian H1N1, and human H3N2) [2] transmitted to humans. During 16 months of the outbreak, 284,000 deaths including 201,200 respiratory deaths and 83,300 cardiovascular disease deaths associated with H1N1 infections were reported by the US Centers for Disease Control and Prevention (CDC). As a result, influenza has drawn an extraordinary level of attention with concerns about the ability to respond to an influenza pandemic on a national and international scale. The availability of effective means of flu surveillance is critical for the control of influenza virus infection. [3] To this end, point-of-care (POC) diagnosis for influenza is vital in administration of therapeutics and prevention of virus outbreaks, yet current POC diagnostic tests have relatively poor performance and are in need of further development. The focus of this work, therefore, is to develop a POC detection method for influenza A virus that overcomes the limitations of current approaches on sensitivity, limit of detection (LOD), ease of use, and assay time.

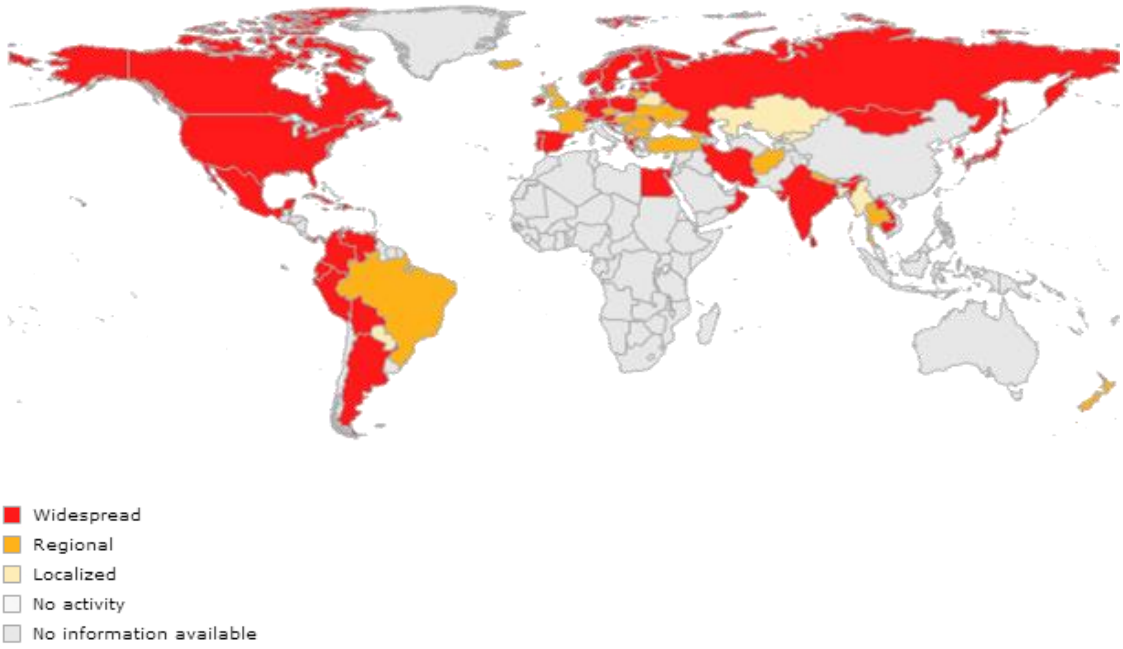

Figure 1. The weekly influenza surveillance report on Nov 2009 when the outbreak was at its peak. This map indicates geographic spread and does not measure the severity of influenza activity. Adapted with permission from *WHO.int* Apr. 2015 [4].

Influenza Virus

Influenza viruses are RNA viruses, i.e. RNA as their genetic materials, and are classified as influenza virus type A, B, and C, which share many similarities in overall structure. Influenza viruses infect a wide range of host animals including humans, pigs, horses, dogs, and aquatic birds; of which pigs are the natural reservoir of all influenza A subtypes. [1b, 5] The type A viruses are the most virulent human pathogens among the three influenza types and cause the most severe disease. Influenza A viruses are roughly spherical of 80-120 nm in diameter. Two glycoproteins, hemagglutinin (HA) and neuraminidase (NA) (Figure 2), are abundantly distributed on the virus particle surface, playing significant roles in the infection cycle of the viruses.[6] HA contributes to high

pathogenicity of the virus in many animal species and initiates the entry of the virion while NA plays a key role in the budding process of the newly formed virion from the host cell. Based on the distribution and functions of HA and NA, researchers target them for certain purposes. A number of polyclonal and/or monoclonal antibodies are generated to selectively bind to different HA serotypes and they can be employed to detect and differentiate influenza A subtypes and strains.

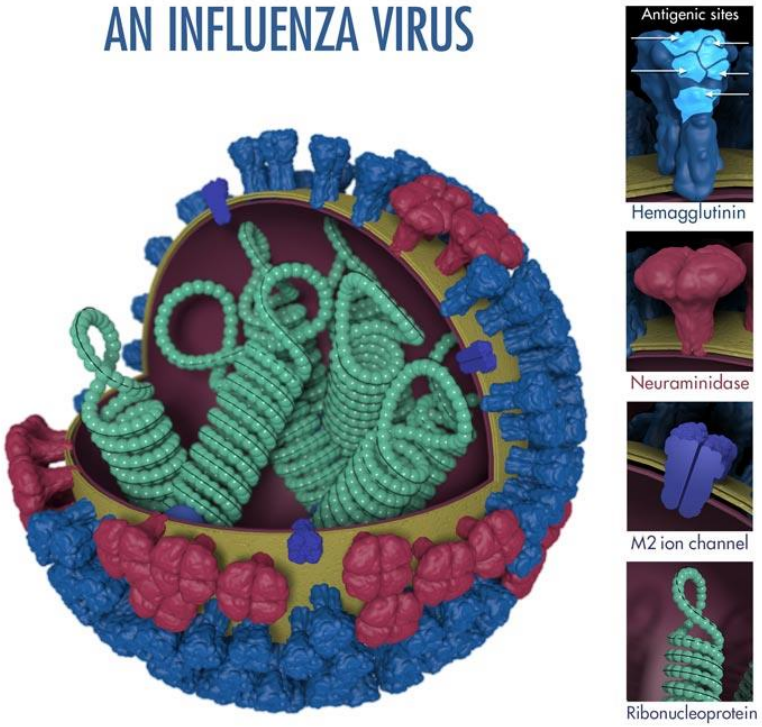

Figure 2. Different features of an influenza virus particle, including two surface proteins HA (in blue) and NA (in red). Adapted with permission from *CDC.gov. Apr. 2015* [7].

Traditional and Current Influenza Virus Detection Platforms

Virus culture [8], nucleic acid testing [3, 9], and immunoassays [10] are primary detection approaches to confirm acute human influenza virus infection. These three platforms possess different extents of analytical sensitivities and specificities. The selection of an appropriate method also greatly depends on technical diagnostic variables such as required turnaround time, available technical expertise, and financial resources. Indeed, there is no single method satisfying all the desired criteria.

Virus isolation in cell culture has been employed in infection diagnosis since its discovery in the early 1960s and drastic expansion in the early 1970s. [8b] Despite technological advances in more modern detection platforms, virus culture still serves as the standard for virus detection and a reference point for all other methods. A specimen after collection and processing is introduced to a cell culture monolayer and allowed to incubate for days to weeks until degenerative changes or cytopathogenic effects (CPE) in the monolayer cells are observed. Characteristics of CPE (i.e. swelling, shrinking, rounding of cells to clustering, syncytium formation, and total damage of the monolayer), infected cell types, specimen collected sites, and length of time to CPE are the criteria used to predict the type of virus present. For influenza viruses A and B in particular, CPE is slowly or not apparently expressed in primary culture. Another test, hemadsorption (HAD), is performed afterwards. Infected cells generate and express viral hemagglutinin proteins on their plasma membranes. These proteins can be detected by their formation of clumps with erythrocytes in the HAD test. It is worth noting that besides influenza viruses A and B, parainfluenza virus and mumps virus are positive with HAD as well. Thus, additional confirmatory testing is required. [8b] Virus isolation in cell culture

provides a great capacity to detect multiple viruses yet is time-consuming, expertise demanding, and limited to laboratory examination (in other words not feasible for routine diagnostic testing).

Nucleic acid testing, especially RT-PCR (reverse-transcriptase polymerase chain reaction) [9] has been developed and applied to speed viral detection. This platform can be utilized separately or in combination with virus culture to identify viruses. The target viral RNA strands of influenza A viruses in clinical samples or in cell culture supernatants are isolated, reverse translated to complementary DNA and amplified to generate a larger number of copies for detection using gel electrophoresis. Hence, even at a low concentration of virus in the specimen, remarkable sensitivity is still provided. Furthermore, assay time is significantly reduced to several hours. Nucleic acid testing platforms, thus, have been applied broadly in a variety of applications in research and clinical diagnostics for most known viruses. Nevertheless, the performance of PCR-based methods significantly depends on viral nucleic acid extraction, primer and probe design, and technical expertise. The cost for instruments varies from $5,000 to more than $50,000, plus additional expenses for reagents [8b]. As a result, many POC facilities have limited access to this technology because of limited resources.

Immunoassays (IAs), on the other hands, are known for availability, specificity, and versatility, and therefore have become a centerpiece in diagnostics [11]. IAs are bioanalytical methods to examine the presence or concentration of macromolecules (or analytes), utilizing immunoglobulins, also called antibodies. These assays have been engineered and innovated to maximize the simplicity of use and speed of the assays so that they are not limited to lab-based testing but can also be operated in the field for POC

testing.[11b, 12] To date, IAs remain the most widely used POC diagnostic platform. However, this convenience comes at the expense of assay sensitivity. With that said, a part of the work presented in this thesis is dedicated to the improvement of IA sensitivity. Key terms and characteristics of IAs will be addressed in greater details in the following sections.

Immunoassay Fundamentals

Immunoassay Compositions: Antibody

As dictated in the name of the platform, it goes without saying that antibodies play a central role in IAs. Antibodies (Abs), also known as immunoglobulins are glycoprotein molecules produced by plasma cells (white blood cells). They are critical to the response of the immune system to antigens such as bacteria and viruses. Among the 5 classes of antibodies (including IgM, IgD, IgG, IgA, and IgE), IgG is the most common one used in IAs. An IgG molecule is a large Y-shaped protein, constructed by basic components, two large heavy chains and two small light chains held together by disulfide bonds (Figure 3). [13] The two identical arms of the Y-shaped protein are termed Fab fragments for fragment antigen binding, while the stem is named Fc for fragment crystallizable. Antibodies recognize pathogens such as bacteria and viruses by specifically binding to antigens (targeted molecules of antibodies) on bacteria or viruses. Each tip on the two arms of the Y is a paratope, which is similarly analogous to a lock, specific to an epitope on the antigen, which is also analogous to a key. These two structures (a paratope and an epitope) are spatially complementary, hence, bind together with high precision. IgG is further classified into different subclasses based on subtle alterations confined to the Fc portion. For the purpose of detecting influenza A virus, IgG

antibodies are used to specifically target hemagglutinin or HA proteins expressed abundantly on the surface of the virus particle. In this case, HAs act as epitopes of the virus. With various strains of influenza A, HA proteins are subtly different; thus, the IgG antibodies are selectively generated in correspondence to each HA subtype.

Antibodies can be either polyclonal or monoclonal. Figure 4 demonstrates the difference between the two terms. The former one is used to define a pool of antibodies with different paratopes, which target multiple epitopes on an antigen. The latter one describes a pool of antibodies with identical paratopes, which target a single epitope on an antigen. Depending on the analysis purposes, polyclonal or monoclonal antibodies are preferred. Polyclonal antibodies are usually more cost-effective and better in overall affinity due to multiple binding sites whilst monoclonal antibodies possess a higher level of specificity owing to unique antibody-antigen interaction. [14]

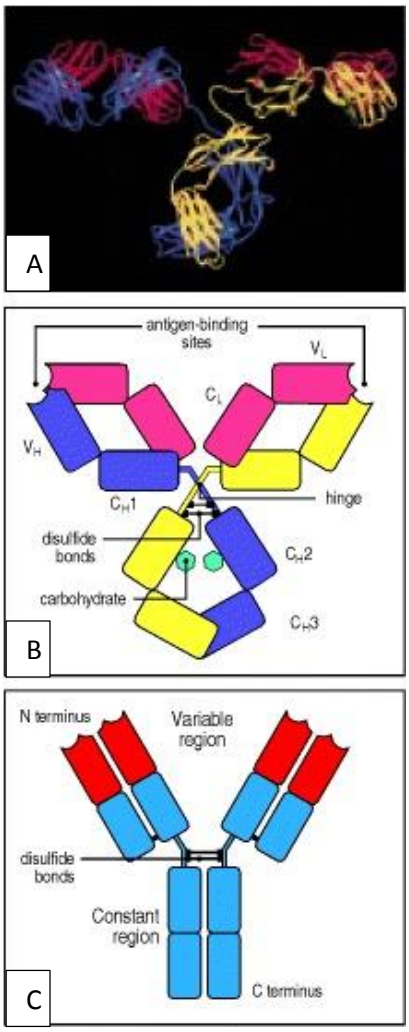

Figure 3. (A) Spatial structure of an antibody molecule. (B) Fundamental components of an antibody molecule including heavy chains (in yellow and blue) and light chains (in pink). (C) Fab and Fc fragment breakdown. Adapted with permission from Janeway *et al.* 2001 [13].

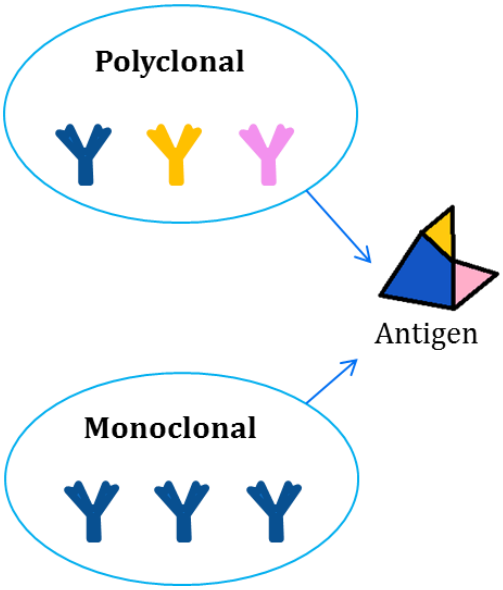

Figure 4. Polyclonal antibodies are a collection of immunoglobulin molecules that react against a specific antigen; each antibody recognizes a different epitope (demonstrated as color coded species). Monoclonal antibodies are monospecific antibodies that target a single epitope of a specific antigen.

Immunoassay Compositions: Signal Generators

A signal generator is the second essential component of an immunoassay in addition to antibodies. In immunoassays, antibodies are often modified with some signal generating labels so that the complex formed between antibody and antigen is determined by measuring the labels' properties such as radioactivity, enzyme activity, light absorption or emission or scattering, etc. These labels provide magnified signals therefore significantly enhance the sensitivity of the detection. Some common immunoassay labels are radioactive labels [15] and non-radioactive labels including enzymes [11a, 16], fluorescent probes [17], chemiluminescent compounds [18], and nanoparticle labels [10d, 19], etc. Radioactive labels offer outstanding sensitivity, however possess health and safety risks.

Consequently, radio immunoassays are not ubiquitously used for analysis nowadays and are replaced by other assays with non-radioactive labels. Even though these alternative labels provide relatively sufficient sensitivity, most of the assays utilizing them are restricted to lab-based analysis due to the non-portability of the instruments used for detecting generated signals. Moreover, these labels are not capable of multiplexed detection.

Immunoassay Formats

IAs are generally classified as heterogeneous and homogeneous assays (Figure 5A and 5B, respectively). Heterogeneous IAs require the removal of unbound antigen and antibody from the surface of a substrate on which the reaction occurs. For instance, when implementing an direct ELISA (enzyme-linked immunoassay) [20], a representative of heterogeneous assays, samples containing targeted antigen are loaded onto separate wells (usually in a 96-well polystyrene plate) and incubated for 4 to 24 hr. The unbound antigen is washed from the surface. A solution of non-reacting protein, such as bovine serum albumin or casein, is added to the well in order to block any plastic surface in the well, which remains uncoated by the antigen. The following step is the introduction of a primary antibody linked to an enzyme, which is specific to the antigen. Another 4 hr is consumed on incubation, and then the excess antibody is removed from the well plate. A substrate of the enzyme is added and the reaction between the substrate and enzyme produces a colored product, which indicates the presence of the antigen. UV-Vis instruments can measure the color change; the intensity of the color is correlated to the concentration of the antigen. If the antigen is absent, there should not be any change in color. A heterogeneous IA is a lengthy process with multiple cycles of incubation and

rinsing, therefore is time and labor intensive. A primary reason for long incubation time is that the binding between antibody and antigen (as macro-biomolecules) is limited by small diffusional coefficients of the antigen when delivered to the sensing surface.[5b]

Homogeneous assays (Figure 5B) are another option for immunoassay format. Antibody molecules are immobilized onto mobile carriers, e.g. gold nanoparticles [12, 21]. The conjugated particles then are mixed with the sample containing analytes, leading to the formation of sandwiched antibody-antigen-antibody complex in solution. Gold nanoparticles function as signal transducers, rendering changes in optical properties to indicate the occurrence of antibody-antigen binding events. In contrast to heterogeneous format, no separation of unbound reagents is required in homogeneous assays. Multiple washing cycles are eliminated from homogeneous assay protocols; the incubation time is short, usually in a few minutes owing to fast solution phase kinetics. [10d, 19c] Thus, it is less time and labor consuming to employ this format. Nevertheless, there are limited readout technologies that have been developed for homogeneous IAs.

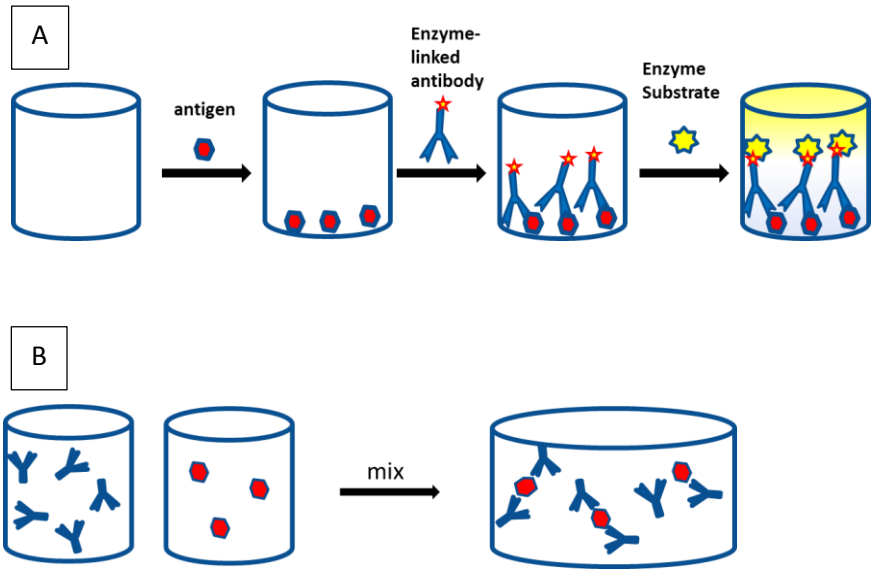

Figure 5. Schematic illustration of (A) heterogeneous immunoassays and (B) homogeneous immunoassays.

Immunochromatographic Assays

Immumochromatographic assays or lateral flow assays (LFAs) are heterogeneous assays engineered to overcome time and labor of conventional heterogeneous assays.

Figure 6 shows the configuration that describes the generic mechanism of how a LFA works. [22] Three different antibodies employed in the configuration are detection antibody (specific binding to antigen), capture antibody (specific binding to antigen), and anti-detection antibody (specific binding to the detection antibody). There are five primary compartments composing an immunochomatographic system including sample application pad, reagent pad (containing detection antibody labeled with latex beads or gold colloids), test line (at which capture antibody is immobilized), control line (having anti-detection antibody attached to the surface), and absorption pad (functioning as a waste chamber and creating capillary driving force) (Figure 6A). Samples containing

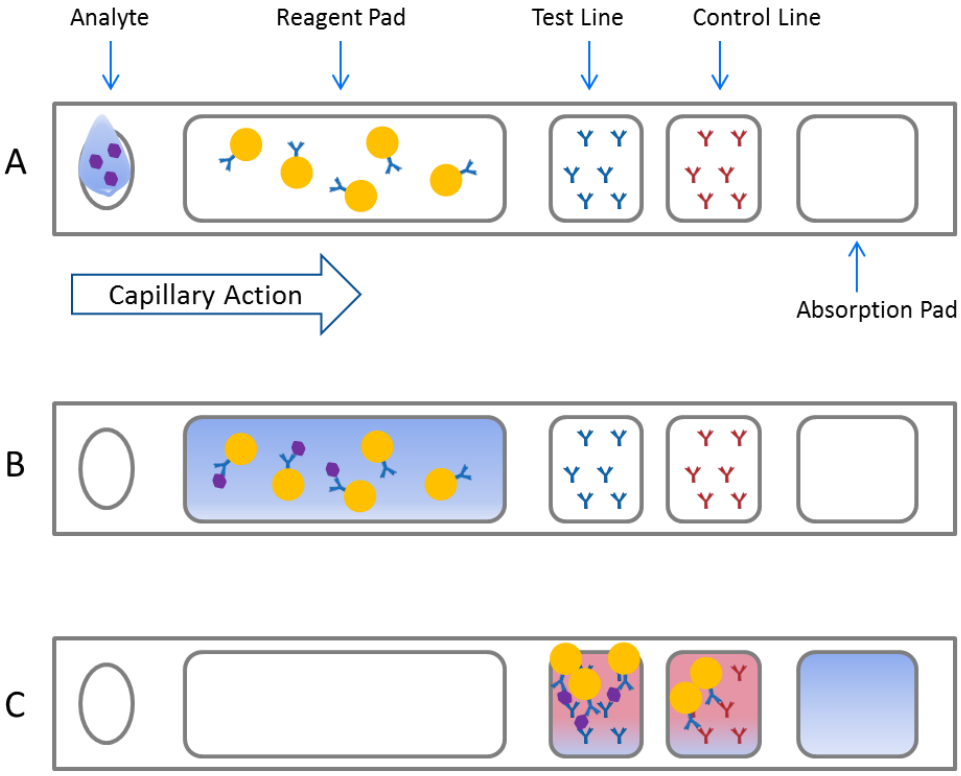

Figure 6. Schematic illustration of immunochromatographic assays. (A) A sample is applied at the sample application pad, (B) The sample travels to the reagent pad, and (C) The sample arrives at the test line. Redrew from O'Farrell *et al.* 2009 [23]

analytes/virus are collected and prepared in an aqueous medium and applied at the sample application pad. The aliquot is drawn along the stick by capillary action and travels to the reagent pad. The detection antibody with gold colloid label is placed in a dehydrated state in the reagent pad and restored to active form by dissolving in the aqueous medium. The detection antibody possesses paratopes that bind to distinct epitopes of the antigen on the analyte; a complex of antigen-detection antibody is formed (Figure 6B). The complex and the unreacted reagent (detection antibody-gold colloid labels) continue flowing to the test line, at which only the complex of antigen-detection

antibody is captured via specific interaction of the antigen to the capture antibody. The unreacted labels pass through the test line to the control line and are anchored there. The accumulations of gold-colloids at both lines produce a distinct red color to indicate a positive test for antigen. One red line only at the test line indicate a negative sample (Figure 6C). The control line indicates proper sample flow. LFAs typically provide yes/no responses but some efforts are put in to obtain semi-quantification. It is worth noting that the color change of the test line depends on the concentration of antigen and the binding of the antigen to detection antibody and capture antibody. False negative results are often caused at the early or late stage of infection when the level of virus in the body is relatively low. Even though LFAs are relatively efficient in terms of cost, simplicity, and speed, their poor detection limit is a major limitation. The sensitivity of rapid antigen tests validated using PCR assays demonstrates a significant variation of 39-80% [24]. Furthermore, LFAs are currently limited to singleplexed detection. With that said, the next generation of rapid tests for influenza detection should be focused on addressing the detection limit (LOD) and multiplexing challenges.

Functionalized Gold Nanoparticles for Bio-Detection

Nanoparticles are defined as nanomaterial having the average diameter no greater than 100 nm [25]. Among them, gold nanoparticles (AuNPs) are the most extensively investigated due to their unique optical properties, which can be utilized as a label in various applications such as sensing and imaging. AuNPs provide an outstanding platform in developing analytical methods for biosensing in nanoscale owing to size-tunable properties and extremely large scattering cross-section to facilitate highly sensitive multiplexed detection. The modification of the AuNP surface can be tailored to

meet the requirements for specific applications, e.g. biosensors, by coating AuNPs with a bio-recognition element such as an antibody. When AuNPs are used as labels in IAs, detection can be achieved by a change in the intensity or peak position of optical absorption, fluorescence emission, reflection, surface plasmon resonance (SPR), surface enhanced Raman scattering (SERS), and dynamic light scattering (DLS). The majority of AuNP assays are the heterogeneous format. While providing high sensitivity, they still require long assay time and many laborious steps. An alternative format is homogeneous IAs but they are limited in the readout technology. In this regard, DLS has emerged as a promising detection method for homogeneous AuNP-based assays. The principles of DLS and its application for AuNP bioconjugation monitoring and aggregate detection in homogeneous AuNP-based assays will be discussed in the following section.

AuNP-based biosensors are prepared via various immobilization techniques of the biomolecules to the particles' surface. The active conformations of the biomolecules when adsorbed on AuNPs directly affect both stability of the biosensors and reproducibility of signals. AuNPs possessing a high surface-to-volume ratio lead to a large amount of biological molecules (e.g. antibody) can be immobilized on the surface. Direct adsorption is fast; it can take place on the order of seconds. Biomolecules can easily adsorb through electrostatic interaction and protect AuNPs from aggregation in high saline concentration environment of real biological samples. However, there is no control over the orientation of adsorbed molecules; therefore, the activity of the biomolecule after immobilization is not guaranteed. Moreover, it has been suggested that the weakly adsorbed biomolecules can desorb from the particle surface since the molecule is not covalently attached. [26] An alternative way to avoid the likelihood of

antibody desorption is to covalent attach antibody to the AuNP surfaces via linker molecules. [27] Biofunctional linkers that have anchor groups such as thiols, disulfides, or phosphine ligands are often used for their binding to Au. The other end of the linkers is covalently coupled with biological molecules via carbodiimide, succinimide, maleidiimide functional groups. Regarding the effort to manage the proper orientation of antibody on the particle surface, protein A or protein G has been utilized by some research groups as cross-linkers for antibody. [19c, 28] In the scope of this thesis, the two former methods of modification were utilized in correspondence to a specific goal for each project.

Dynamic Light Scattering for AuNP Probe Assembly and Aggregates Detection

AuNPs are known to have a large light absorption and scattering cross section. Dynamic light scattering (DLS) is a technique used widely for particle size and size distribution studies based on the light scattering property and the Brownian motion of spherical particles (Figure 7). The size of the particles is calculated according to the Stokes-Einstein relation and Doppler shift of the incident laser beam after interacting with moving particles [29]. The advancement in development of recent DLS instruments offers benefits of low cost and low maintenance. In comparison to other methods, monitoring AuNPs via DLS is simply done with higher sensitivity and in a timely manner.

DLS has been successfully developed to monitor and characterize biomolecule-AuNP conjugation in situ according to Jans et al. 2009 [54]. DLS can readily measure a small change of 3-5 nm for a 100 nm diameter nanoparticle. Kinetic studies of protein-AuNP surface (e.g. protein A adsorption) and protein-protein (e.g. protein A-human IgG)

interactions can also be obtained via DLS. [54] The adsorption process of proteins was observed as the growth of AuNP in size over time during incubation. As the diameter of the particle increases, the particle diffusion is reduced in the suspension (according to Stoke-Einstein equation). When the particle reaches the maximum growth of the monolayer (complete coverage), the stability of the AuNP probes can be tested in high salt content environment. [51, 54] If the conjugate is not stable after adding salt, DLS readout indicates a dramatic change in size (at least more than double the size of a

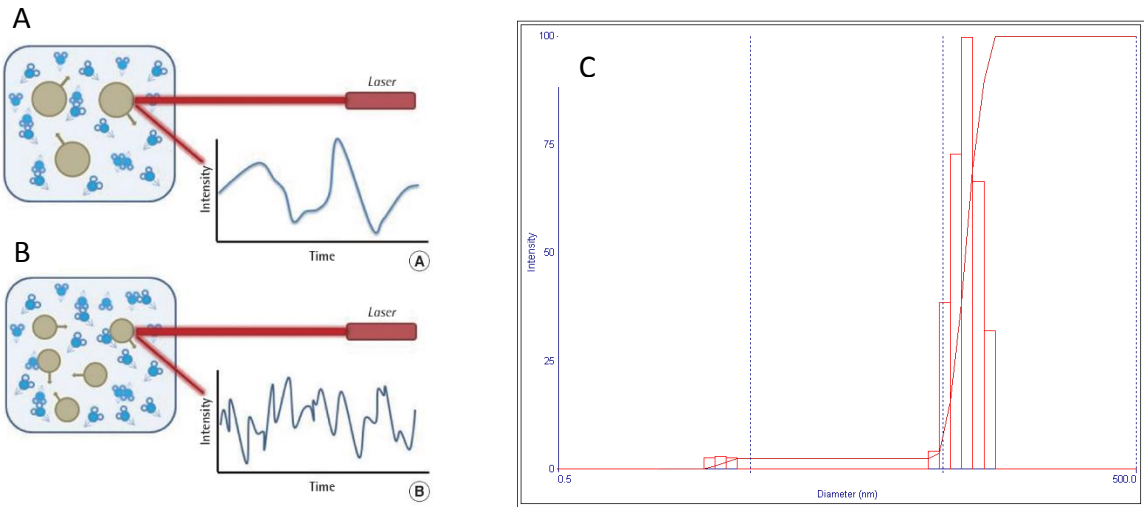

Figure 7. Dynamic light scattering principle for (A) large particles and (B) small particles; larger particles produce more scattering light. Adapted with permission from Kim *et al.* 2014 [30]. (C) A hydrodynamic diameter distribution histogram of a DLS reading for 60 nm AuNP.

free particle). Also as stated in Jans *et al.* 2009 [31], the size increment of a full layer of IgG molecules on AuNP is 15-20 nm regardless the particle size.

Based on the same principle, the correlation between diffusion rate and particle size, DLS can differentiate individual nanoparticles versus nanoparticle dimers,

oligomers or aggregates in solution. DLS is capable of detecting nanoparticle aggregates at low analyte concentration (high pg/mL to low ng/mL). [32] DLS was reported to be used in a homogeneous AuNP-based IAs for cancer biomarker detection for the first time in Liu *et al.* 2008 [33]. Free prostate specific antigen (f-PSA) was targeted as a biomarker for prostate cancer diagnosis. Two different monoclonal anti-PSA antibodies were used to detect f-PSA; one of them works as a capture antibody while the other one functions as a detector antibody. Each antibody specifically binds to a single epitope on the antigen; therefore, it takes a pair of one capture antibody and one detector antibody to form a sandwich complex with a prostate antigen molecule. For the AuNP probes preparation, the detector Ab was immobilized on citrate-caped Au nanospheres as it binds better to negatively charge surface. Whereas, the capture Ab favors the positively charged surface so it was attached to cetyltrimethyl ammonium bromide (CTAB)-coated Au nanorods. These two probes were prepared separately prior to mixing with the sample containing f-PSA. The interactions of the capture Ab and f-PSA and detector Ab induced aggregation of Au nanospheres and Au nanorods, which is detected via DLS. It was reported in the paper that an unknown sample of 0.5 ng/mL f-PSA was determined via the DLS assay. Yet, they did not report the LOD.

In Driskell *et al.* 2011, the homogeneous AuNP-based IA coupled with DLS was adapted to detect influenza A virus with slight modifications. [10d] It was proposed in the study that the DLS assay works better for larger targets such as viruses since they have multiple epitopes to form more contact with Ab-assembled AuNP. Different from Liu *et al.* 2008, only one type of AuNP probes was synthesized using Au nanospheres and one monoclonal antibody specific to native HA from one particular influenza A virus strain.

This protocol is versatile and highly adaptable to detect a different strain of influenza virus when a monoclonal antibody specific to the corresponding HA protein is available to use. The multiple copies of HA abundantly distributed on the virus particle provide more access for the antibody on AuNP probes to come into contact. Less time and labor are consumed in AuNP probe assembly since one type of probe is needed. The simplicity of DLS detection based on size change is a merit yet becomes a disadvantage for developing multiplexed detection since no differentiation between aggregates of different AuNP-Ab probes for different virus strains is obtained.

Surface-Enhanced Raman Scattering (SERS) Biosensors

Raman spectroscopy is a technique that is associated to inelastic scattering of monochromatic light. Raman effects refer to the frequency of the scattered photons shifted up and down relative to incident light. The difference between excitation and emission wavelength is called Stokes shift. This shift provides information about vibrational, rotational, and other low-frequency transitions in molecules. Whereas most of the scattered photons conserve the same energy of the incident ones (Rayleigh scattering), a small fraction of them is scattered either at higher (anti Stokes scattering) or lower (Stokes scattering) energy levels (example of Rhodamine 6G spectra in Figure 8). [27b] The spectroscopic vibrational fingerprint of the investigated molecule is the collection of the scattered photons corresponding to the energy difference between vibrational states in the molecule. Raman (both anti-Stokes and Stokes) scattering is inherently weak and it is difficult to separate the weak inelastically scattering light from the intense Rayleigh scattered light. The applications of Raman scattering has been expanded since the discovery of SERS by Fleischmann *et al.* in 1974. [34] Raman signal can be enhanced by a

factor as much as 10^9 when the analyte is adsorbed onto nanostructured-metals that have high optical reflectivity such as silver, gold, and copper. According to electromagnetic theory, the size of the metal particles is required to be much smaller than the wavelength of the exciting radiation, usually in 10-80 nm range. That explains why AuNPs are perfect substrates for SERS. In addition, SERS enhancement is even greater for nanoparticles in an aggregated state with small gaps between them. [27b, 35] The gaps, also called hot spots, enhance the light scattering efficacy of the analyte once they are small enough for plasmon coupling between particles to occur. The SERS signal of the investigated molecule when located in the gap is drastically increased. [27b, 35a]

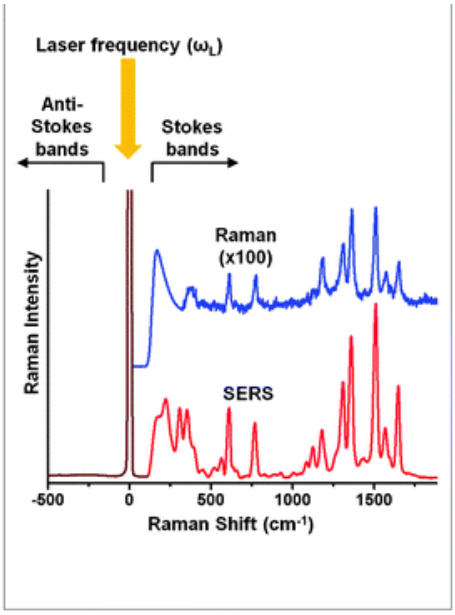

Figure 8. Normal Raman spectrum of Rhodamine 6G 10^{-3} M in nanopure water (blue line) multiplied by a factor of 100 and SERS spectrum of Rhodamine 6G 10^{-7} M on silver colloid under the same experimental conditions. Adapted from Guerrini *et al* 2012. [27b]

As stated above, distinct vibrational profiles for each molecule provided by SERS make this technique ideal for detection of multiple analytes in a mixture due to the sharp fingerprint spectra. The combination of SERS with immunoassays utilizing antibody-conjugated gold nanoparticles (Ab-AuNPs) is promising for a multiplexed detection technique providing high sensitivity (down to single molecule detection [36]) and specificity (distinction of different strains of a single virus type [36a]). SERS itself serves as a powerful analytical tool to provide detailed information at the molecular level. In order to enhance the specificity of the detection, antibodies with high selectivity are immobilized onto nanostructured surfaces to only target the antigen of interest in complex biological matrix. Although the signal obtained from a biomolecule absorbed on a roughened metallic surface or trapped between nanoparticles is significantly enhanced relative to original Raman signals, the high protein content nature of biological matrix still interfere with SERS analysis. Therefore, extrinsic labels, aromatic compounds with intrinsically strong Raman scattering, are utilized as signal generators to amplify the binding event of interest and alleviate background signals. [36b] AuNP probes having extrinsic labels attached are referred to as extrinsic Raman labels (or ERLs). Remarkable efforts have been paid to develop a platform for SERS multiplexed detection such as the work done by Wang *et al.* 2009. [26] The group reported they were able to detect four different IgG antigens simultaneously in a single heterogeneous sandwiched IA. However, the assay setup falls back to inherent limitations of the heterogeneous format, i.e. a tedious protocol with long incubation times and multiple washing cycles.

Thesis Objective

Based on preliminary studies and literature research, the focus of this thesis is to investigate a gold nanoparticle-based homogeneous immunoassay and SERS for read-out to develop a multiplexed and POC detection platform for influenza A virus. This method is pursued to overcome the existing drawbacks of current rapid antigen testing kits, namely sensitivity and multiplexing.

Research Overview

In this study gold nanoparticles are utilized as carriers for antibody as well as labels for detection. (1) AuNP probes are prepared by immobilization of antibody on the gold surface of the particle. The modification process is monitored by size measuring via DLS. Antibody molecules bind directly on the gold nanoparticles to form a full layer (Figure 9A). (2) After the preparation of AuNP probes, a homogenous immunoassay is carried out by mixing a specimen with the AuNP probes without pre-treating the sample. Antibodies bind to HA protein on the virion and cross-link AuNPs to produce aggregation in solution (Figure 9B). The level of aggregation corresponds to virus concentration. Thus, the detection of virus is actually the matter of detecting the nanoparticle aggregates. (3) Aggregates of particles can be detected based on sizing measurement via DLS since clusters of AuNP have a bigger size compared to the free AuNP probes. (4) A second technique, which can be employed to detect the aggregates, is SERS. To this end, an extra step needs to be added to the preparation of particle assembly; Raman reporter molecules are attached to the AuNP probes, which are now referred as extrinsic Raman labels (ERLs) (Figure 9A). Once aggregation is induced by the introduction of virus, AuNPs are brought into close proximity with each other and

form small gaps in between them. The Raman reporters are trapped in the gaps producing strong Raman scattering when dehydrated on a filter membrane and excited with a laser beam (Figure 9C). There is direct correlation between the concentration of virus and the intensity of Raman signal provided by the Raman reporter. (5) Toward the ultimate goal of our research group, the assay platform employing SERS can be developed to perform multiplexed detection when multiple ERLs are synthesized using different antibodies targeting different strains of virus and distinct Raman label molecules correspondingly assigned to each antibody (Figure 10).

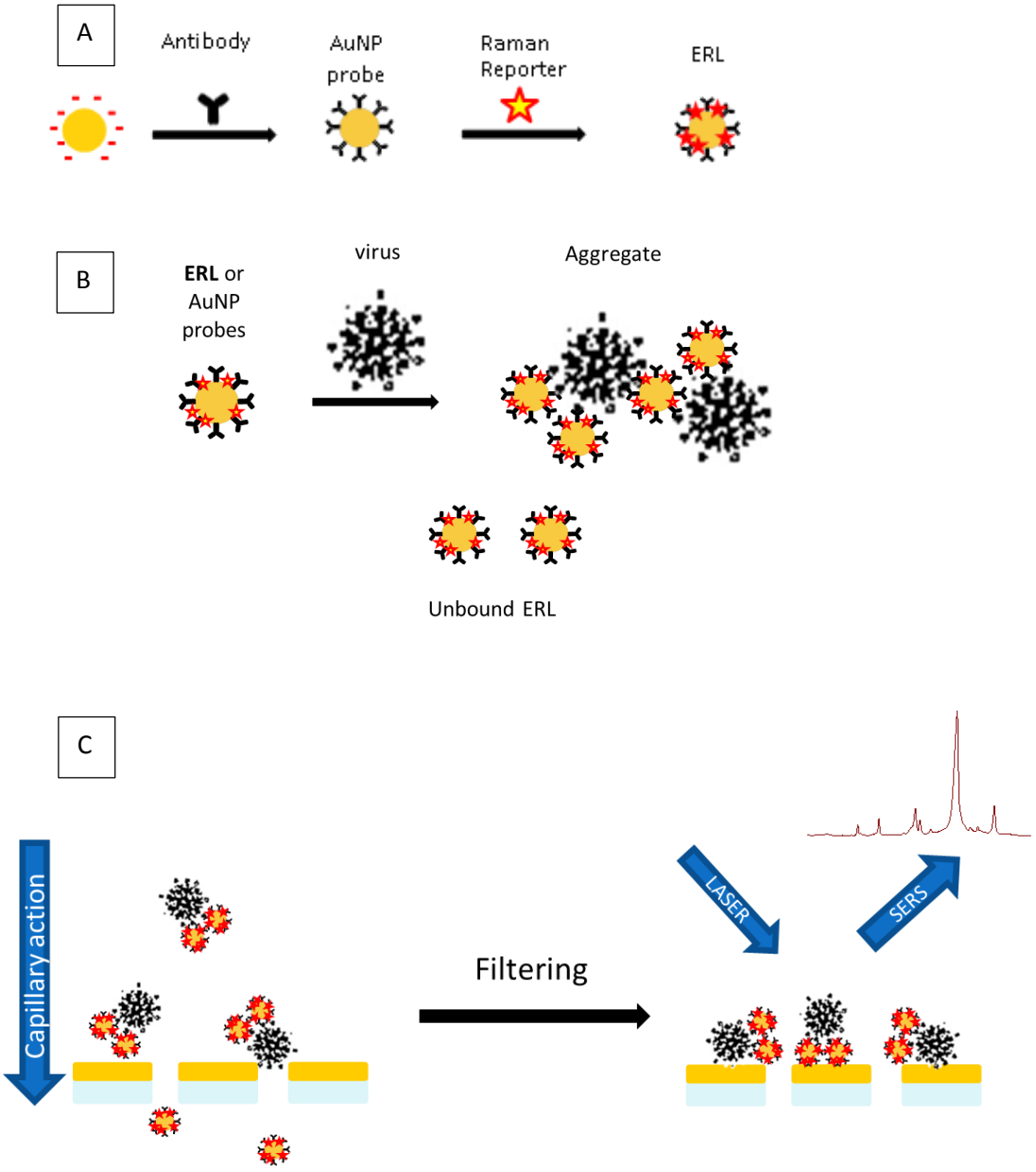

Figure 9. Schematic illustration of one-step homogeneous immunoassay coupled with SERS analysis. (A) Immobilization of Raman reporter and antibody molecules to synthesize AuNP probes or ERLs, (B) Virus-induced aggregation of ERLs in solution, (C) Filtration to separate aggregates from unbound ERLs to concentrate SERS signals.

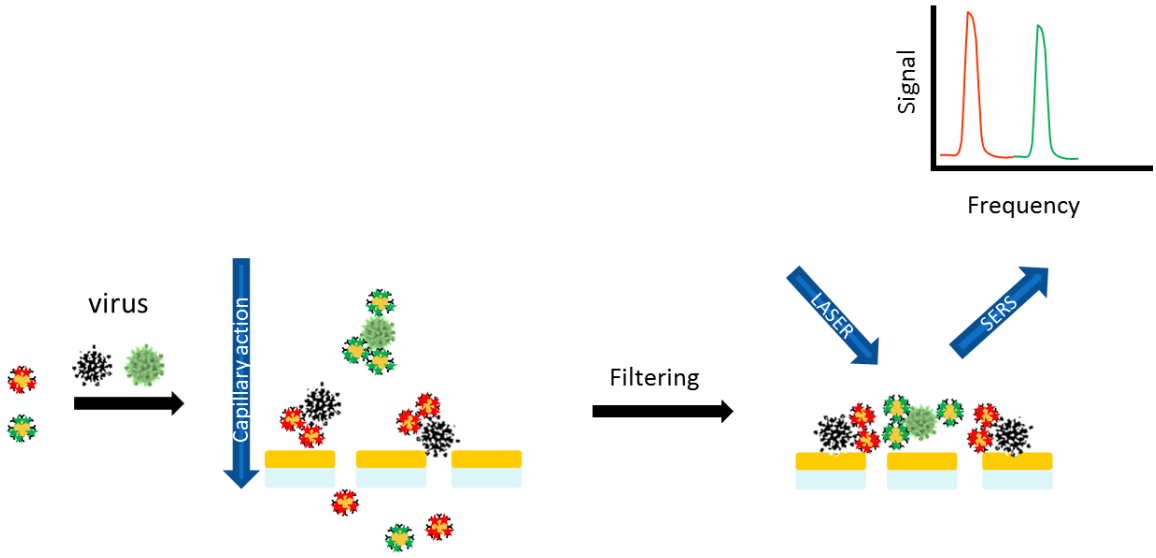

Figure 10. Schematic illustration of SERS homogeneous multiplexed immunoassay. Multiplexed detection can be carried out when multiple types of ERLs targeting different strains of virus are used.

CHAPTER II

RAPID SCREENING OF ANTIBODY-ANTIGEN BINDING USING DYNAMIC LIGHT SCATTERING (DLS) AND GOLD NANOPARTICLES

This study has been published in the journal *Analytical Methods* as Lai, Y. H.; Koo, S.; Oh, S. H.; Driskell, E. A.; & Driskell, J. D. Rapid Screening of Antibody-Antigen Binding Using Dynamic Light Scattering (DLS) and Gold Nanoparticles. *Analytical Methods*. **2015**, ***7***, 7249-7255 [37].

Introduction

Nanoparticle–based immunoassays have emerged as a great tool for rapid, sensitive, and low-cost point of care diagnostic tests due to the selective molecular recognition based on antibody-antigen specificity and unique properties of nanoparticles (NP). Antibodies are immobilized onto the surface of nanoparticles that vary in material, size, and shape which can be tailored to improve the detection of pathogens and biomarkers. Despite the advantages provided by NPs and readout technology, detection improvement is also inherently governed by the antibody. There is a direct correlation between assay performance and antibody affinity, regardless of the readout technology.

Advances in genetic engineering of antibodies have led to the development of many recombinant monoclonal antibodies (mAb) highly specific to many targets. In antibody engineering and production, several antibody selection platforms such as phage/ribosome and mRNA/microbial cell displays, [38] flow cytometry, [39] and protein

arrays, [40] have been employed to isolate potential antibodies for maturation and to build an antibody library for target binding. As an outcome of the selection process, a mixture of antibody clones needs to be individually analyzed to obtain certain target binding properties. Additionally, many mAbs developed using traditional means (i.e. hybridomas) are commercially available yet vendors provide little information on antibody affinity. Thus, the burden to evaluate mAb affinity and specificity falls on the user to identify the most appropriate mAb candidate for a particular study, and the ability to rank the affinity of mAbs in addition to specificity towards the molecule of interest becomes essential.

Enzyme-linked immunosorbent assay (ELISA) is a primary method to screen the specificity and affinity of mAbs. [38b] ELISA has many attributes such as sensitivity due to enzyme driven amplification, and low cost of analysis; [11a, 16] however, it possesses certain limitations. For example, ELISAs require multiple steps of incubation and washing cycles that are labor-intensive and time-consuming. Moreover, results are often irreproducible and matrix dependent because plasma constituents often impact enzyme activity. A single ELISA assay usually takes up to 24 h for analysis; a major portion of assay time is consumed by incubation due to small diffusion coefficients of biomacromolecules.

Additional challenges may be encountered when an ELISA is used to screen antibodies to be incorporated into emerging AuNP-based immunoassays. Conjugation of the antibody to AuNPs may affect the bioactivity of the antibody which will not be detected by ELISA. Thus, ELISA may not accurately select for the most suitable antibody in AuNP-based immunoassays. An alternative method to screen and characterize mAbs that overcomes the limitations of ELISA is needed.

Herein a rapid screening method for determining antibody-antigen binding specificity and affinity was developed using AuNPs and dynamic light scattering (DLS). Briefly, AuNP probes are produced by the immobilization of antibodies onto AuNP. The probes are then mixed with the specimen, and the presence of the target antigen induces aggregation of the AuNP probe. The formation of aggregates is detected as an increase in hydrodynamic diameter by the DLS instrument with high sensitivity. [31, 33, 41] To develop the DLS-based mAb screening method and establish proof-of-principle, four anti-influenza virus monoclonal antibodies were directly adsorbed onto the surface of AuNP. Each of the antibodies was developed against influenza virus A/New Caledonia/20/99 and directed towards the H1 hemagglutinin, a surface protein on the virus. Next, a series of dilutions of the corresponding antigen (influenza virus A/New Caledonia/20/99 (H1N1)) was mixed with the AuNP probes. Calibration curves for each of the antibodies were constructed to rank the specificity and affinity of their binding. Owing to single-step and wash-free procedure, the screening time using DLS was significantly reduced to 30 min in comparison to 24 h by ELISA.

Experimental

Reagents

Gold nanoparticles (60 nm; 2.6×10^{10} particles/mL) were purchased from Ted Pella, Inc (Redding, CA). Phosphate buffered saline (PBS) was purchased from Thermo Scientific (Logan, UT). Borate buffers were prepared from sodium borate obtained from Fisher Scientific (Fair Lawn, NJ). Bovine serum albumin (BSA) was purchased from Sigma (St. Louis, MO).

Antibodies

Mouse monoclonal anti-influenza A antibodies (InA4, InA16, InA88, and InA97) specific to native HA from influenza virus A/New Caledonia/20/99 (H1N1) were purchased from Novus Biological. The antibodies were purified by protein A affinity chromatography and supplied in PBS, pH 7.4.

Viruses

Two independently prepared virus samples were used, one was propagated in-house (UIUC) and a second stock was graciously provided by collaborators at the University of Georgia (UGA).

Human influenza virus isolates (both H1N1 subtypes) A/New Caledonia/20/99 and A/Puerto Rico/8/34 were grown in 9 to 11-day old embryonated chicken eggs for 48 to 72 hours at 37 °C. Fertile eggs were obtained from a flock of specific pathogen-free leghorn chickens (Merial Select, Gainesville, GA and Sunrise Farms, Catskill, NY). Allantoic fluid from infected eggs was then collected and pooled for each strain, divided into aliquots, and stored at -80 °C. The 50% tissue culture infectious dose ($TCID_{50}$) of the stock viruses was determined by the Reed and Meunch method on MDCK cells. [42] A/New Caledonia/20/99 (UGA) titer was 1.75×10^7 $TCID_{50}$/mL and A/New Caledonia/20/99 (UIUC) was 3.00×10^5 $TCID_{50}$/mL. A/Puerto Rico/8/34titer was 3.70×10^7 $TCID_{50}$/mL.

Optimization of pH for AuNP-mAb Conjugation

A 100 µL aliquot of 60 nm gold nanoparticle suspension was added to separate 0.50 mL microcentrifuge tubes (5 tubes in total). The pH of the colloidal gold sol was adjusted to 5.5, 6.5, 7.5, 8.5, or 9.5 by adding 4 µL of 50 mM phosphate buffer pH 5.5,

6.5, and 7.5, and borate buffer 8.5 and 9.5 into each tube, respectively. The antibody (30 µg/mL) was mixed with the pH adjusted suspension 15 min. DLS was used to monitor the hydrodynamic diameter of the particles. A 10 µL aliquot of 10% (wt/v) NaCl was added to each tube to verify the stability of AuNP conjugates in saline environment. [43] DLS measurement was conducted again to determine the appropriate pH for stabilization.

Optimization of Ab Concentration for AuNP-mAb Conjugation

A 100 µL aliquot of 60 nm gold nanoparticle suspension was added to separate 0.50 mL microcentrifuge tubes (11 tubes in total). The pH of the colloidal gold was adjusted to optimal pH by adding 4 µL of 50 mM borate buffer at the optimal pH into each tube. Different amounts of the antibody were added into each tube to obtain a wide range of concentrations (namely, 0, 5.0, 10.0, 15.0, 20.0, 30.0, 40.0, 50.0, 60.0, 70.0, 80.0, 90.0, 100.0, 110.0 µg/mL). The solutions were mixed well. After 15 min, the hydrodynamic diameter of antibody-conjugated AuNPs was measured via DLS. Next, 10 µL of 10% (wt/v) NaCl was added to each tube to verify the stability of AuNP conjugates in saline environment.[43] The changes in size of the particles were measured again by DLS. The amount of antibody added at the stabilization point plus 10% should be used to produce the final antibody-AuNP conjugate. [28b]

Preparation and Characterization of Ab-AuNP

A 4 µL aliquot of 50 mM borate buffer (at the optimal pH for the antibody adsorption) was added to 100 µL AuNP to adjust the pH. The stabilization amount of mAb plus an additional 10% was added to the AuNP for 15 min. A 33 µL aliquot of 1% BSA in borate buffer or phosphate buffer (at the optimal pH for the antibody absorption, 2 mM) was added to bring the concentration of BSA to 0.25% in the Ab-AuNP

suspension. BSA helps to further stabilize the sol against aggregation and also blocks nonspecific binding sites. After 5 min, excess antibody was removed via centrifugation at 5,000 rpm for 5 min. The conjugate was resuspended in100 µL PBS (pH 7.4, 10 mM) with 0.25% BSA to mimic physiological conditions and promote mAb-virus binding.

Immunoassay Protocol

A previously described procedure for the assay was used with slight modifications. [10d] Four-fold serial dilutions of virus stocks were prepared in 10 mM PBS (pH 7.4). A total of 90 µL of virus dilutions were added per well of a 96-well round-bottom microliter plate (Corning, Corning, NY). PBS served as negative control. A 10 µL aliquot of antibody-modified gold nanoparticles made by the above procedure was added to each well and allowed to incubate for 30 min at room temperature. The AuNP reagent/sample mixture was then transferred to a 70 µL small volume disposable cuvette (Eppendorf, Germany) for DLS measurement.

DLS Measurement

A BI-90Plus (Brookhaven Instruments Corporation, NY) equipped with a 658 nm laser and avalanche photodiode detector (Perkin) was used to measure hydrodynamic diameters of AuNP for all DLS measurements. The backscattered light collection angle was set at 90°. Each sample was analyzed in triplicate and each measurement was an average of three 30-s runs. Data were collected and analyzed using MAS OPTION particle sizing software. Hydrodynamic diameters were referred to as the effective diameter by cumulants analysis.

ELISA

All the ELISA experiments were conducted by Koo S. and Oh S. H., our collaborators at UIUC.

Virus (diluted 1:100) or PBS (negative control) was added, 100 µL per well in a 96 well Immulon 2HB microtiter plate, and incubated 18 hours at 4 °C. Wells were washed and then blocked with BSA/non-fat milk. Serial dilutions (1:4) of anti-influenza mAbs were applied to pre-adsorbed plates, starting with a dilution of 1:100. After washing, HRP labelled goat anti-mouse IgG (Thermo-Fisher) was applied as the secondary antibody, 1:1000, to all wells. After the final washing step, 1-step Turbo TMB ELISA (Thermo-Fisher) was added for the substrate and the reaction was stopped with 1M H_2SO_4. Absorbance was measured at 450 nm on a 96-well format plate reader (SpectraMax Gemini reader and SpectraMax software). Absorbance readings for mAbs against PBS were subtracted from absorbance readings for mAbs against virus and plotted.

Results and Discussion

Adsorption of Proteins onto Gold Nanoparticles

One major concern relating to any AuNP–based immunoassay is the stability of antibody-AuNP conjugates in biological environments of high ionic strength. Antibodies can be immobilized onto a gold surface via a cross-linker or directly adsorbed to the surface. Regardless of the immobilization strategy, the conjugate needs to be protected from salt-induced aggregation. [44] In this study, direct adsorption was applied. The behaviors of different subclasses of antibody in the direct conjugation are distinct. [43] The direct adsorption of proteins onto the gold surface is a complex process dependent on

several parameters such as the concentration, isoelectric point of protein, bound fraction of segments, ionic strength, and pH. [19c, 28b, 45] However, it is not practical to simultaneously study all the factors for the optimization of this process. Herein DLS was employed to investigate the immobilization of mouse monoclonal IgG1 (InA4 and InA97) and IgG2 antibodies (InA88 and InA16) on gold nanoparticles primarily in relation to pH and concentration of the protein; the other parameters will be correspondingly discussed.

The pH has great influence on the hydrogen bonds and overall charge of the biomacromolecule. Extremely high or low pH can cause a dramatic change in molecular configuration and perhaps its bioactivity. Therefore, the pH range selected for this study was 5.5 to 9.5, which minimizes the likelihood of damage to the molecular activity. It is well established that the pH slightly above or equal to isoelectric point of the biomolecule is the optimal pH for protein adsorption. [45] However, we suggest that the pH dependent study is more broadly applicable since the surface charge distribution is necessary to be taken into account. Zhang *et al.* 2014 indicated that proteins and AuNP can be alike in charge at a certain pH and still interact with each other, e.g. negatively charged BSA, can still interact with citrate–capped gold particles via its positive patches. [46]

Previous studies by our group and others suggest 30 µg/mL IgG will fully coat AuNP. [19c, 47] Therefore, as a starting point to investigate pH dependent adsorption, 60 nm AuNP were mixed well with each antibody (30 µg/mL) at the adjusted pH. DLS was used to measure the mean hydrodynamic diameter (D_H) and monitor antibody adsorption. The adsorption curve for InA4, plotted as D_H versus pH is displayed in Figure 11A. Adsorption of the antibody caused the D_H to increase by 10 nm to 40 nm, depending on

the pH, relative to the unconjugated AuNP. We have previously demonstrated that D_H increases by ~20 nm when the AuNP is fully saturated with a layer of antibody. [19c] Thus, we speculate that at pH 5.5, in which the D_H increased by 40 nm, the charge of the antibody was sufficiently positive that the antibody itself destabilized the AuNP to induce aggregation. Conversely, at pH 9.5, in which the D_H only increased by 10 nm, the antibody had sufficient negative charge that a full monolayer of antibody was not adsorbed on the negatively charged citrate-capped AuNP. NaCl was then added to a final concentration of 1% (wt/v) to confirm antibody adsorption and establish stability of the conjugate in a solution of high ionic strength. Figure 11A shows the D_H as a function of pH for the InA4-AuNP conjugate after the addition of NaCl. It is evident that at the extreme pHs, e.g., 5.5 and 9.5, not enough antibody adsorbed onto the AuNP to render the particles stable. However, at pH 8.0 the InA4-AuNP conjugates were least affected by the electrolytes and the data confirm complete antibody adsorption for stability. Additional antibody-AuNP conjugates were prepared with three other antibodies and the coagulation curves for the conjugates in a saline environment are provided in Figure 11B. The adsorption of IgG1 antibodies (InA4 and InA97) were highly unstable at pH lower than 6.5. InA97 was quite stable at pH higher than 6.5 whilst InA4 reached the smallest diameter of 107 nm at only pH 8.0 (the expected diameter of AuNP-InA4 is ~80 to 90 nm). It is worth mentioning that the stability of InA4-AuNP conjugate was not obtained at the optimal pH since the adsorption also relies on a sufficient amount of antibody required for full protection. This will be further discussed in the following section. As for IgG2 (InA16 and InA88), the stability of nanoparticles after adsorption did not undergo such a dramatic change for the tested pH range (Figure 11B). The adsorption of IgG2 was

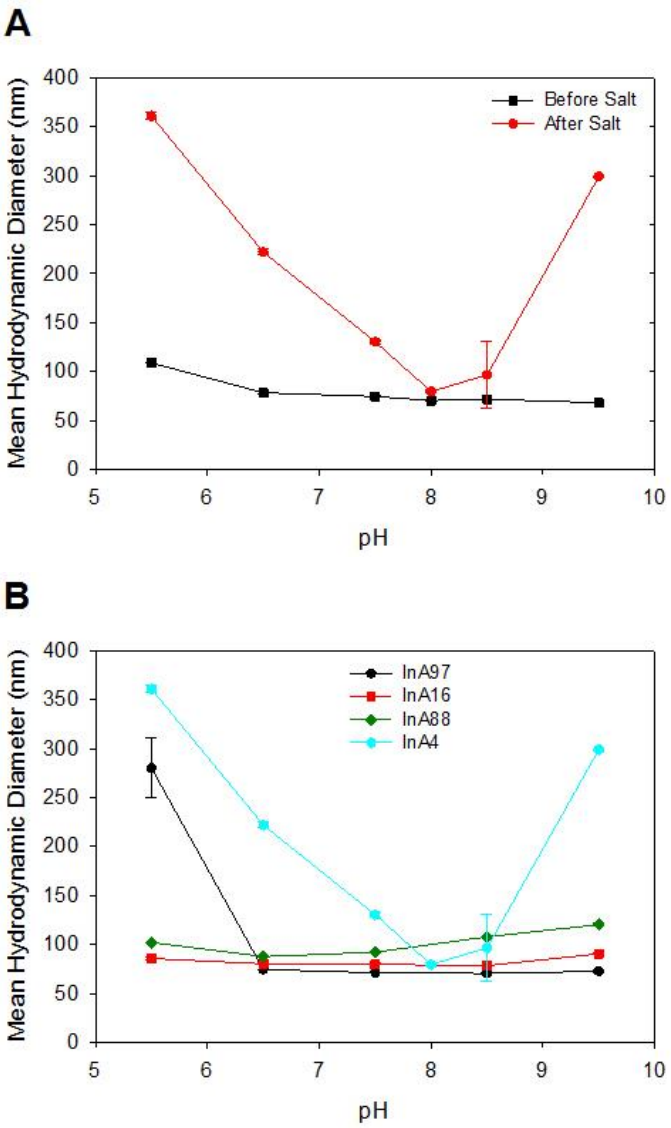

Figure 11. DLS aggregation curves to assess pH-dependent adsorption of mAb onto AuNP. The mAb concentration is fixed at 30 µg/mL. (A) Mean hydrodynamic diameter of InA4-AuNP conjugate as a function of pH before and after addition of 1% NaCl. (B) Mean hydrodynamic diameter of four mAb-AuNP conjugate as a function of pH after addition of 1% NaCl. Each data point is the average of 3 independent experiments with standard deviations presented by error bars.

optimized at pH 6.5-7.5. These results showed good agreement with the optimal pH for

IgG subtypes adsorbed on gold nano particle concluded by William *et al.* 1980. [43]

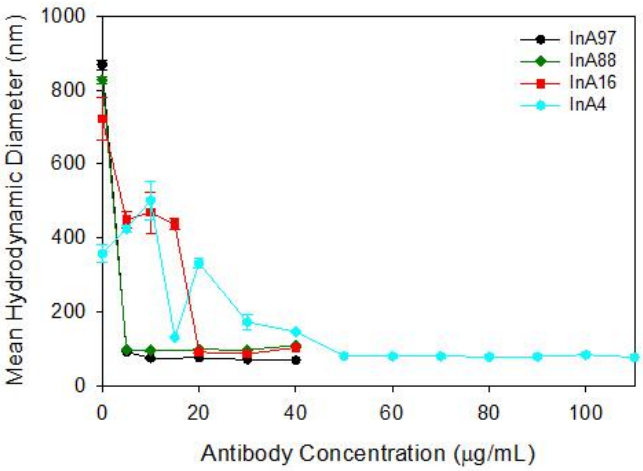

Figure 12. Mean hydrodynamic diameter of mAb-AuNP conjugates as a function of mAb concentration after the addition of 1% NaCl.

In addition to pH, the adsorption and subsequent stabilization of gold nanoparticles are also affected by antibody concentration. To determine the minimum amount of antibody required for adsorption and stabilization of AuNP, various amounts of antibody (0-110 µg/mL) were incubated for 15 min with AuNP adjusted to the optimal mAb-dependent pH, followed by the addition of NaCl. DLS was then used to measure the D_H as a means of evaluating AuNP-antibody stability (Figure 12). At optimal pH, InA97 and InA88 only required 5.0 µg of antibody per ml of AuNP to protect against salt-induced aggregation and the stability was also maintained at higher concentrations of the antibody. A slightly greater concentration of InA16 was required for stabilization (20 µg/ml) while InA4 required 50 µg/mL to stabilize the gold suspension. It is likely that InA97, A16, and A88 have confirmations that form more contacts with the gold surface so that the surface rapidly reaches saturation by these antibodies at lower coverage. On

the other hand, InA4 has fewer contacts to the gold surface per molecule.

It was reported that the addition of 110% of the minimum amount of antibody is sufficient for conjugate stabilization. [28b] In general, it is more favorable to use a secondary stabilizer such as BSA to obtain the desired stability of the colloidal gold conjugation in saline environment for longer storage time due to steric stabilization created by the double layer. [45] Therefore, to prepare AuNP probes for use in DLS assays, the AuNP suspension was adjusted to the optimal pH, the requisite amount of antibody was mixed with colloidal gold, and 0.25% (wt/v) BSA was added to the suspension without the removal of excess antibody. Centrifugation before adding BSA may bring the antibody-AuNP proximal to each other and cross-link therefore is not recommended. Zhang *et al.* 2014 reported that IgG molecules displace citrate ligands during adsorption and BSA forms a monolayer and stabilizes the antibody-nanoparticle conjugate by its electrostatic interaction to the antibody monolayer. [46] The unbound antibodies were then removed by centrifugation three times and the colloidal gold nanoparticles were resuspended in PBS (10 mM) buffer containing 0.25% (wt/v) BSA. No significant increase in size indicated that the conjugate was stable in the saline solution. The conjugates were stored at 4 °C for 5 days without aggregation or a loss in activity.

Validating DLS Assay to Monitor Antibody-Antigen Binding

To establish this platform as a means of monitoring antibody-antigen interaction, AuNPs were modified with the mAb InA97 using the optimized conjugation procedure detailed in the previous section. The InA97-AuNP probes suspended in PBS measured 83 nm in diameter via DLS, consistent with the expected size of a 60 nm AuNP coated with a protective IgG layer. The InA97-AuNP probes were mixed with dilutions of influenza

A/New Caledonia virus or PBS, e.g. negative control, for 30 min and the mean hydrodynamic diameter (D_H) was measured via DLS. The calibration curve, constructed as a plot of D_H increase versus virus concentration, is displayed in Figure 13. Figure 13

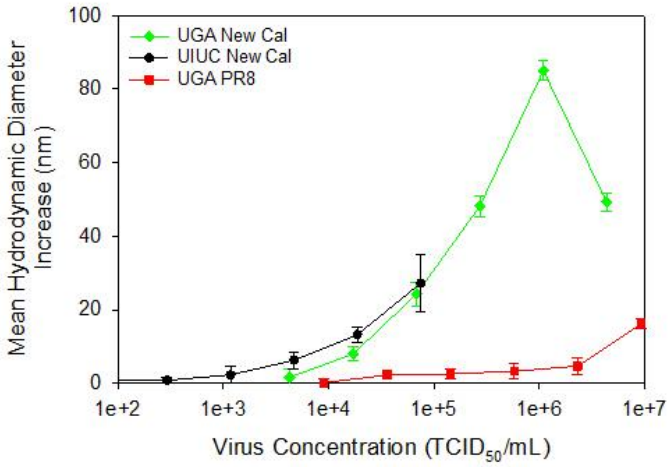

Figure 13. DLS response curves to evaluate the specific binding of influenza A viruses with InA97-AuNP probes. Two assays were performed on independent preparations of New Caledonia virus and one assay was performed on the PR8 strain of influenza virus. Each data point is the average of 3 independent experiments with standard deviations presented by error bars.

shows a detectable increase in D_H relative to the D_H of the InA97-AuNP probe at a New Caledonia virus concentration of 10^3 $TCID_{50}$/mL. Moreover, the increase in D_H correlates with an increase in New Caledonia virus concentration reaching a maximum value at a virus concentration of 10^6 $TCID_{50}$/mL. The "hook effect" was observed at the highest concentration of New Caledonia virus as a decrease in diameter. This phenomenon was previously reported and discussed in detail for DLS assays. [10d, 32]

The robustness of the assay was evaluated by analyzing a second, independently

prepared New Caledonia virus stock. This virus was propagated using the same procedure and yielded a viral titer of 3.00×10^5 $TCID_{50}$/mL. InA97-AuNP probes were mixed with 4-fold dilutions of this New Caledonia stock and DLS was used to measure the formation of aggregates resulting from virus-antibody binding. The results are displayed in Figure 13 and the measured D_H provided a similar concentration-dependent response to that obtained for the original virus stock.

Upon mixing the InA97-AuNP probes with influenza A/Puerto Rico/8/34 virus, no significant aggregates were detected via DLS (Figure 13). It is worth noting that a slight increase in D_H was measured for InA97 probes when mixed with the highest concentration of influenza A/Puerto Rico/8/34 virus. It is possible that this increase is due to a specific or non-specific interaction between this strain of influenza virus and InA97, albeit very weak (low K_a). However, it is more likely that the increase in D_H at this virus concentration is caused by the matrix. While AuNP is highly efficient at light scattering and is the primary source of light scattering in the DLS measurement, [48] the high concentrations of large particulate in undiluted allantoic fluid is likely the cause of the measured increase in D_H for this concentration. Thus, we conclude that the InA97 mAb selectively binds influenza A/New Caledonia virus and does not have an affinity for influenza A/Puerto Rico/8/34 virus.

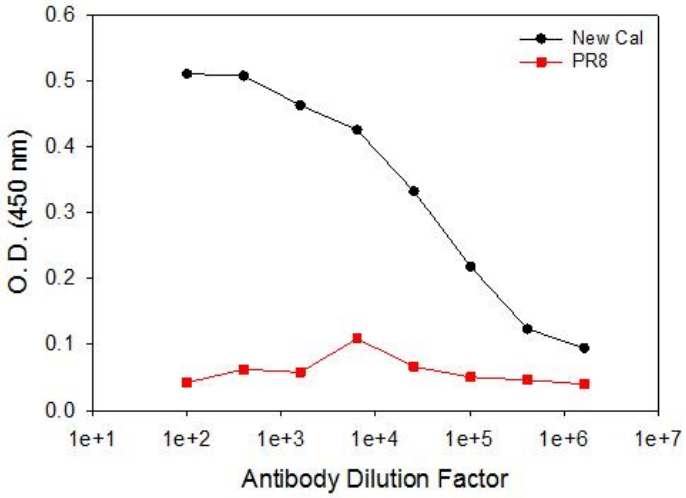

Figure 14. ELISA results to evaluate InA97 binding specificity towards New Caledonia and PR8 strains of influenza A viruses. The data were collected by our collaborators at UIUC.

ELISA is the gold standard platform for testing antibody-antigen binding. Therefore, an ELISA was performed by our collaborators at UIUC to evaluate the binding of InA97 to New Caledonia and PR8 viruses, and the results were compared to the DLS-derived binding specificity results. The ELISA results are presented in Figure 14. ELISA confirmed that InA97 specifically binds to New Caledonia; however, InA97 does not have a specific interaction with PR8 as minimal binding of the antibody is detected even for high antibody concentrations. These results are in agreement with the DLS results for InA97 binding specificity, and serve as validation of the DLS platform.

Screening and Evaluating Antibody-Virus Binding Specificity

The selection of the antibody is critical to any antibody-based detection method. The assay performance is governed by the antibody-antigen binding; thus, it is essential to understand the specificity and affinity of this interaction. To this end, the DLS assay

was explored as a potential candidate for rapidly screening antibody-antigen specificity and affinity. The antibody-antigen binding assay is reduced to 30 min using the DLS assay compared to 24 h using ELISA. Moreover, the DLS assay may be better suited for rapidly screening antibodies intended for use in AuNP-based immunoassays. During conjugation to AuNP, conformational changes may affect the antibody bioactivity relative to the free antibody that is evaluated for binding in the ELISA format.[49] Thus, this novel DLS-based screening method may be a better alternative to ELISA with respect to time and effectiveness.

Three additional monoclonal anti-influenza antibodies InA4, InA16, and InA88 were investigated to evaluate specific binding interactions with intact influenza A/New Caledonia/20/99 (H1N1). All four antibodies were developed using influenza A/New Caledonia/20/99 as the immunogen and the vendor advertises the antibodies as broadly cross-reactive with H1 subtype influenza viruses. Figure 15A shows the DLS response curves of the four antibody-AuNP probes incubated with 4-fold dilutions of the New Caledonia strain. The extent of aggregation was used to evaluate the interaction between the antibody and the virus. Only InA97 and InA4 antibodies were found to specifically bind to New Caledonia virus. The assay suggests that InA97 had a greater affinity toward

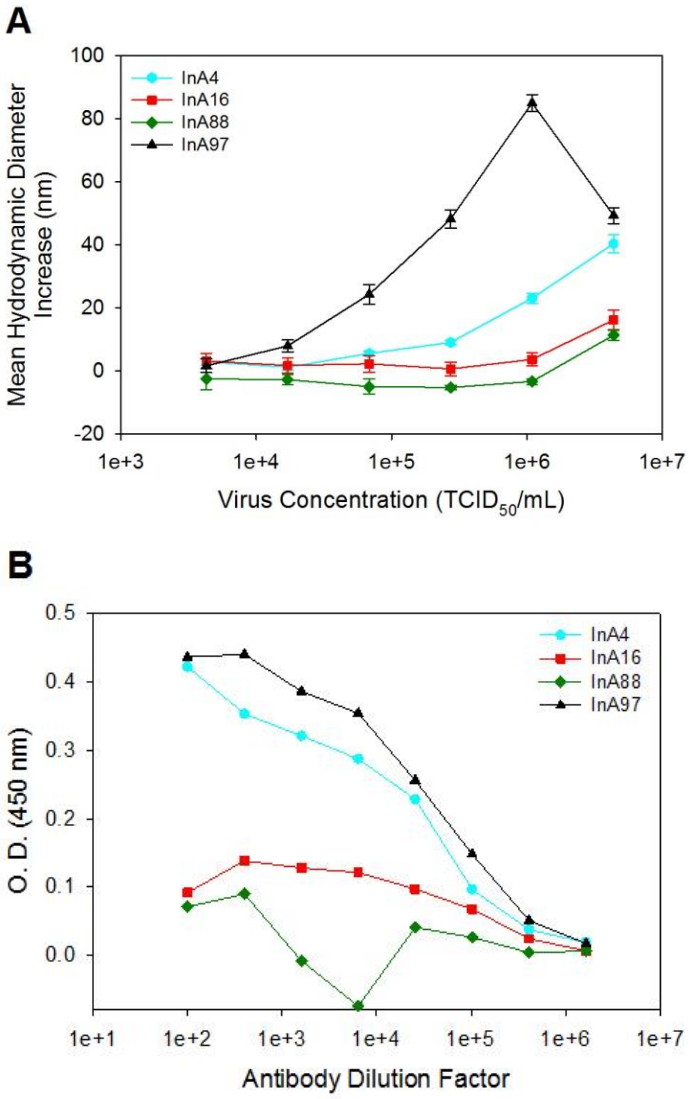

Figure 15. Evaluation of antibody binding to influenza A New Caledonia virus. (A) DLS response curves to evaluate the specific binding of influenza A New Caledonia virus with five Ab-AuNP probes. Each data point is the average of 3 independent experiments with standard deviations presented by error bars. (B) ELISA. The ELISA data were collected by our collaborators at UIUC.

the New Caledonia virus strain compared to InA4, given that aggregation of the InA97-AuNP probes was detected at a lower virus concentration than for the InA4-AuNP

conjugates. Interestingly, no increase in D_H was measured for the antibody-AuNP conjugates for the other two antibodies, InA16 and InA88. The small increase in D_H a the highest concentration of virus was similar for each antibody probe and was likely due to particulate in the undiluted matrix as discussed above. These data suggest that these two antibodies do not specifically bind New Caledonia virus. This is in contrast to the expected results as both of these antibodies were also developed with New Caledonia as the immunogen.

One explanation for the unexpected results is that the InA16 and InA88 antibodies lost bioactivity upon adsorption to the AuNP, but in the unconjugated state do specifically bind to New Caledonia virus. To test this possibility each antibody was evaluated using an ELISA and the results were directly compared to the DLS assay. The ELISA results are presented in Figure 15B. The direct correlation between the mAb dilution and absorbance demonstrate that InA4 and InA97 are the only antibodies that specifically bind New Caledonia virus. These results are consistent with the DLS results, provide evidence that the lack of InA16 and In88 antibody affinity to the immunogen is not a result of conjugation to the AuNP, and ultimately validate DLS as a rapid and effective platform for screening antibody-antigen binding.

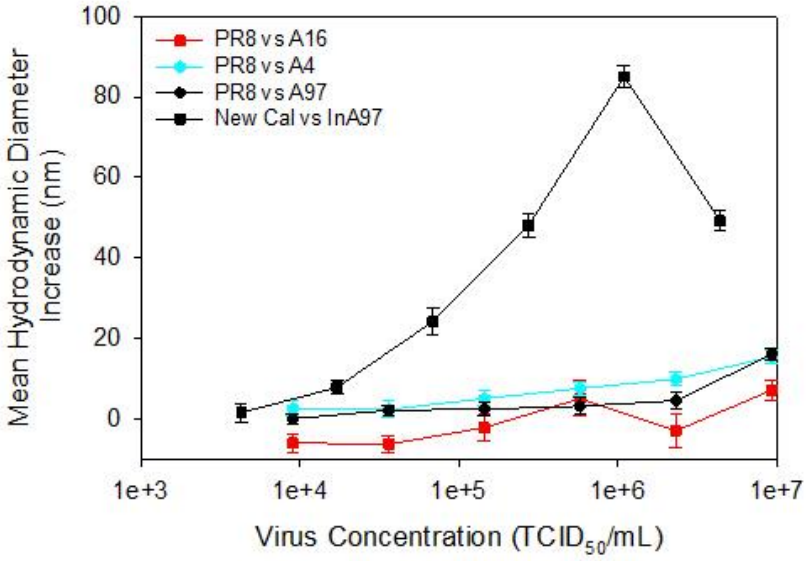

Figure 16. DLS response curves to evaluate the specific binding of influenza A PR/8 virus with four Ab-AuNP probes. The DLS curve for the binding of InA97 to New Caledonia is included as a reference to illustrate specific binding. Each data point is the average of 3 independent experiments with standard deviations presented by error bars.

The DLS assay was also conducted using the three antibody probes and influenza A/PR/8 virus to determine the antibody specificity towards a different H1N1 influenza virus. The DLS response curves are plotted in Figure 16, along with one New Caledonia calibration curve as a point of reference. As is evident in the data, no significant binding of these antibodies to PR8 was detected. While PR8 is the same subtype as New Caledonia, it is not surprising that the antibodies do not bind PR8 as it was not the immunogen used to develop the antibodies. It is probable that the epitopes to which InA97 and InA4 bind are specific to the New Caledonia strain and not conserved across all H1 subtype influenza viruses.

Conclusions

In this investigation, we demonstrate a simple, rapid, and cost–effective method to screen specificity of antibodies in a single–step homogeneous assay using mAb–AuNP probes and DLS. This novel method offers a significant improvement in terms of screening time compared to ELISA assays, while providing the same accurate results as the conventional method. This platform could be easily implemented in most laboratories to select antibodies for a wide variety of targets. This screening method has the potential to expedite the development and optimization of antibody-based diagnostics and antibody therapeutics. In addition, a straightforward protocol to synthesize antibody-AuNP conjugates was presented.

CHAPTER III

SERS-BASED MULTIPLEXED HOMOGENEOUS ASSAY DEVELOPMENT

Overview

As mentioned in the thesis objective, the ultimate goal of our research group is to develop a detection method that can address the issues of sensitivity and multiplexing for POC detection. With that, the third project focusing on multiplexed detection investigation had been launched. The assay platform was developed for mouse IgG, rabbit IgG, and human IgG as model antigens; SERS was used as the primary detection method. The platform, once successfully developed, will be applied to influenza A viruses and other pathogen detection. In the following experiments, polyclonal antibodies were used due to the low-cost and ease of use. The immobilization of these antibodies on AuNPs has been well studied and the binding specificity and selectivity is also known. Therefore, there is no need to go through the processes of optimizing AuNP probe assembly. Yet, the optimization for antibody conjugation and antibody screening (presented in chapter II) will need to be performed when developing the configuration for detecting infectious species, e.g. influenza A viruses, since monoclonal antibodies are usually preferred.

In addition, immobilization of antibody on the AuNP was performed with the assistance of a cross-linker instead of direct adsorption. ERLs, firstly, were produced by coating AuNPs with a monolayer of two thiols (i.e., thiolated Raman reporter molecules

and thiolated cross-linkers). The second thiolate was employed to covalently attach antibody to the particle surface to prevent cross-talk between antibodies from different ERLs in the same suspension. After thiolation, antibodies were attached to the gold surface via the binding to the cross-linker. In this study, goat anti-mouse, goat anti-rabbit, and goat anti-human were utilized. Three ERLs, one with each antibody, were prepared separately before they were mixed together and with the antigens. The procedure was adapted from Wang *et al.* 2009 [26, 50] with modification. Three Raman reporter molecules (or Raman labels) with distinctive spectra were selected. Each of them was assigned to pair with each of the antibodies. The ERLs, after synthesis, were mixed with the specimen. When the antigen bound to its corresponding antibody and induced aggregation, the SERS signal of the corresponding Raman label on the ERLs was turned on. The aggregates were captured by a membrane filter with well-defined pore size while the free ERLs were allowed to flow through. SERS analysis was performed on the membrane filters afterwards since it was proven from Driskell *et al*. 2014 [51] that the aggregates in the dehydrated state provide higher SERS signals (Figure 17).

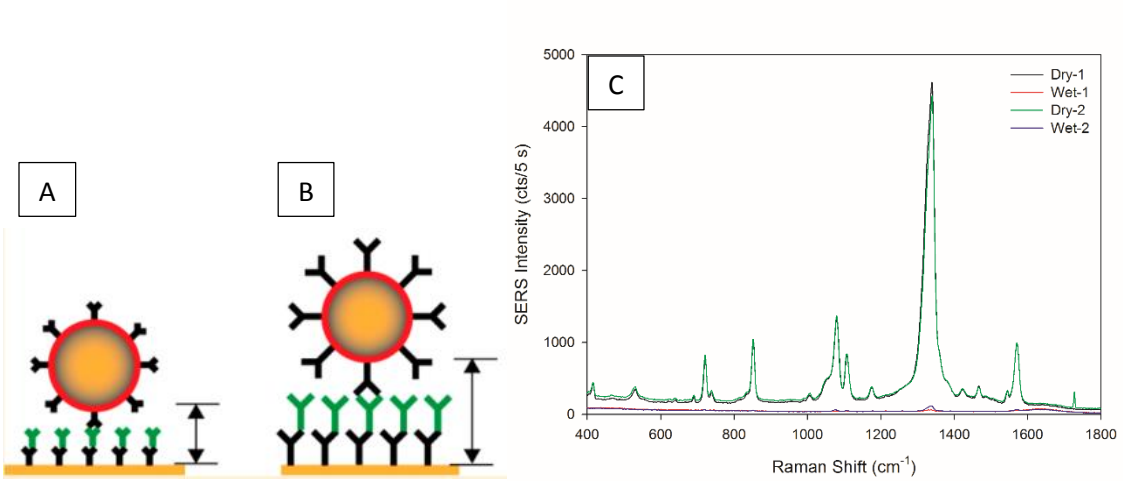

Figure 17. Schematic illustration of the change in the size of the gap between antibody-modified AuNPs and Au surface in accordance to the (A) dehydration and (B) hydration states of the IgG molecules. (C) The SERS responses provided by 4-NBT corresponding to the dry and wet states of the ERLs. There is almost no SERS signal collected from the ERLs when the IgG molecules are hydrated. Adapted with permission from Driskell *et al.* 2014. [51]

Experimental

Reagents and Materials

Gold nanoparticles (80 nm, 1.1 x 10^{10} particles/mL) were purchased from Ted Pella, Inc (Redding, CA). Sodium borate buffer (50 mM, pH 8.96), phosphate-buffered saline (PBS, 10 mM, pH 7.4), goat anti-mouse IgG polyclonal antibody (2 mg/mL), goat anti-rabbit IgG polyclonal antibody (1.7 mg/ mL), goat anti-human polyclonal antibody (1.7 mg/mL), mouse IgG (1.0 mg/mL), rabbit IgG (11.3 mg/mL), and human IgG (2.5 mg/mL) were obtained from Thermo Scientific (Rochford, IL). Bovine serum albumin (BSA), 2-methoxybenzenthiol (2-MeOBT), 4-methoxybenzenthiol (4-MeOBT), 3-methoxybenzenthiol (3-MeOBT), 2-naphthalenethiol (2-NT), 4-nitrobenzenethiol (4-

NBT), 3,3'-dithiobis(sulfosuccinimidyl propionate) (DTSSP) were purchased from Sigma-Aldrich (St. Louis, MO). Polycarbonate track etched (PCTE) membrane filters with a nominal pore diameter of 0.2 μm were purchased from Millipore. All chemicals were analytical grade. All aqueous solutions were prepared with NANO pure deionized water from a Barnstead water purification system (18 MΩ).

Preparation of Extrinsic Raman Labels (ERLs)

ERLs were prepared by co-adsorbing a Raman reporter molecule (i.e. 4-MeOBT or 2-NT or 4-NBT) and DTSSP at the optimal ratio (with the total of 15 nmol for both thiolates) onto gold nanoparticles according to a previously reported procedure, with slight modification [50]. In a microcentrifuge tube, 1000 μL of AuNP was combined with 40 μL 50 mM borate buffer, 12.5 μL thiol mixtures of 1 mM NBT and 1 mM DTSSP; the mixture was incubated for 15 min, and then centrifuge at 5000g for 5 min to remove unbound thiols. The particles were resuspended in 1000 μL 2 mM borate buffer pH 8.5. Next, 16.6 μL goat anti-mouse IgG (or 23.5 μL for goat anti-rabbit or 23.5 μL for goat anti-human) polyclonal antibody was added. The mixture was allowed to incubate overnight on the bench top at room temperature. The ERL suspension was centrifuged at 5000g for 5 min. The supernatant was decanted and the AuNP pellet was resuspended in 1000 μL of 2 mM borate buffer with 1% BSA (pH 8.5). This centrifugation/suspension process was repeated twice more, with the final suspension in 2 mM borate buffer containing 1% BSA and 1% NaCl at pH 8.5.

Antigen-Mediated Assembly and Capture of ERLs

Mouse, rabbit, and human IgG standard solutions were prepared through serial dilutions using PBS. Antigen (10 μL) was introduced to a suspension of ERLs (90 μL) and allowed to incubate at room temperature for one hour. The membrane filters were treated with 200 μL of 1% BSA for 20 min to block non-specific binding. The filtration process was performed via a Bio-Dot microfiltration apparatus. Using a micropipette, 80 μL of the ERL-sample mixture were blotted onto the filter membrane, and then washed with 160 μL of 2 mM borate buffer. Filters were allowed to dry before SERS analysis.

Instrumental Characterization and Assay Readout

Dynamic light scattering was used to monitor the conjugation of antibody onto AuNP and measure the size of the hydrodynamic diameter of antigen-induced aggregates. Measurements were taken with a BI-90 Plus (Brookhaven Instrument Corporation, New York) equipped with a 658-nm laser and an avalanche photodiode laser (Perkin) with the detection angle of backscatterd light set to 90^{o}. The mean hydrodynamic diameter for each sample was averaged from three 30-s runs using MAS OPTION particle sizing software to perform cumulants analysis.

SERS measurements were performed using an Ennwave Optronics, Inc. ProRaman-L-785B Analyzer, using a diode laser at the fixed wavelength 785 nm. The laser was focused to a 100-μm spot with a 10x objective (N.A. 0.52), and the power was adjusted to 10 mW. The instrument was equipped with a high-sensitivity CCD thermoelectrically cooled to -60 ^{o}C. Membrane filters were placed onto a motorized translational stage and tuned to a speed of approximately 0.3 mm/s during 10-s spectral acquisitions. Five spectra were collected at five different locations for each sample.

Sample rastering during spectral acquisition increases sampling area and effectively averages signal from heterogeneous locations to improve signal reproducibility.

Results and Discussion

Assay Design

The intrinsic design of this platform is the employment of gold nanoparticles decorated with Raman active reporters and whole antibody molecules attached via covalent interaction to biofunctional linker molecules (i.e. DTSSP). This configuration of ERLs was slightly different from the classic self-assembly approach, which was presented in chapter II as direct adsorption of antibody on gold surface. The cross-linker molecules with the thiol end binding to gold surface and the other end forming covalent bond to antibody were used instead. The direct adsorption is fast and simple but can be used for singleplexed assays only since the antibody is immobilized via mainly electrostatic force. In multiplexed assays, multiple antibodies are used to assemble ERLs; therefore, covalent linking is essential to minimize the possibility of crosstalk caused by the exchange of antibodies. The use of DTSSP as a cross-linker was anticipated to prevent the cross-talk between different ERLs in the same suspension. [26] In the presence of AuNP in solution, the DTSSP disulfide bond breaks and binds to the gold surface. Each DTSSP molecule provides two binding sites for antibodies on the gold surface. When added in the particle suspension solution, antibodies having primary amine groups perform nucleophilic attack to the succinamidyl ester linkage, break the bond, and form a new amide bond which covalently anchors antibody to the surface (Figure 18).

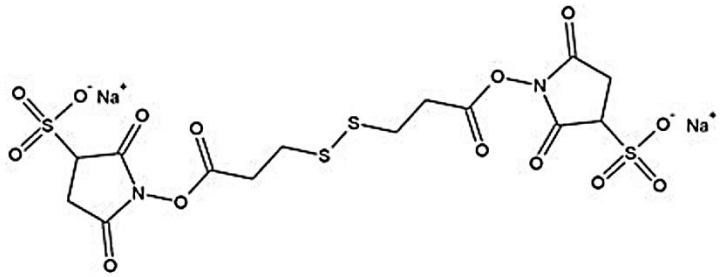

3,3'-dithiobis(sulfosuccinimidyl propionate)

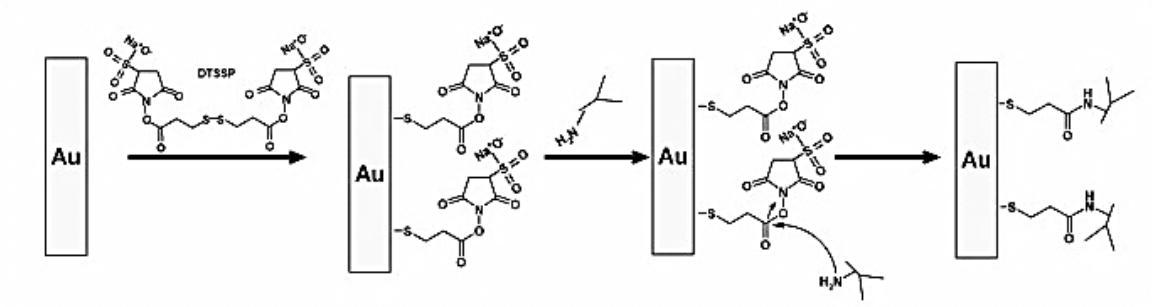

Figure 18. Mechanism of reactions of DTSSP's moieties to Au surface and antibody. Adapted with permission from Escamilla-Gómez *et al.* 2009 [52].

The ERLs, after a complete assembly, were mixed with the specimen containing antigen analytes. Upon the introduction of antigen, the sandwiched antibody-antigen-antibody formation occurred; these interactions brought the nanoparticles close to each other (forming clusters of particles), and creating hot spots for plasmonic coupling inside the cluster. However, in this design whole IgG molecules were used, leading to an interparticle distance of ~21-30 nm according to a previous work done by our group in Driskell *et al.* 2014 [51]. This sufficiently large gap can significantly affect plasmonic coupling efficiency of particles and SERS intensity. In solution, SERS signal can still be measured but the signal-to-background is really low, leading to a compromised sensitivity. An approach to overcome this limitation is to capture the aggregates on a

membrane. By doing this, aggregated ERLs were concentrated and dehydrated; therefore, the interparticle spacing was reduced. Driskell *et al.* 2014 showed that SERS signal can be increased by 50-fold when the aggregate is in dry state versus wet state. It was found that the signal increases when the gaps between particles are small, i.e. antibody and antigen are in dehydrated state (Figure 17).

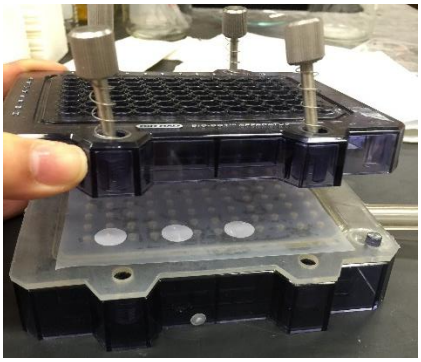

Figure 19. A 48-well Bio-Dot microfiltration apparatus. The apparatus consists of 6 primary components, including sample template with attached sealing screws, parafilm sheet, sealing gasket, gasket support plate, vacuum manifold, and tubing and flow valve.

After allowing for complete aggregation, the solution containing aggregates was transferred for filtration to a 48-well Bio-Dot microfiltration apparatus (Figure 19). Two hundred nm pore size PCTE membrane filters were used for filtration. They were incubated with BSA prior to use to prevent undesired adsorption of unbound ERLs to the surface. The pore size was optimized for capturing both large and small (i.e. dimers or trimers) aggregates formed at even very low concentration of antigen while allowing free ERLs to flow through. The filter membranes with the BSA side facing up were placed underneath the sample template to cover the bottoms of the wells, which had the analyte mixtures added in later (Figure 19). Unused wells were covered by parafilm. The

filtration apparatus was connected to a mini-pump; the suction via vacuum was the driving force for the filtration. With this setting, multiple samples can be filtered simultaneously and separately to save time and avoid cross-contamination. While using 200 nm pore size filter membranes, the optimal size of AuNPs used to prepare ERLs was 80 nm according to Lopez *et al.* 2015. [53]

Only 80 μL of the filtrate solution was needed for the microfiltration apparatus and only 10 μL of specimen was needed for the assay. That means this homogeneous assay can be performed with a very small amount of specimen. In addition, using the vacuum filtration accelerates the filtering process comparing to the apparatus used in Lopez, A. *et al.* 2015. The filtration time was reduced to 15 s including two times of rinsing. Aggregated particles were better concentrated in 3 mm spots via microfiltration apparatus comparing to 4.5 mm spots via home-built apparatus in Lopez *et al.* 2015 [53] (Figure 20).

Figure 20. (A) A home-built blotting apparatus: four sheets of blot paper were layered on the Teflon base and the membrane was placed on top. A rubber O-ring (4-mm inner diameter) was placed between the membrane and top Teflon sheet. (B) the size comparison of two spots of aggregates obtained after filtration via the home-built blotting apparatus (left) and 48-well Bio Dot blotting apparatus (right). Each filter diameter is 13 nm.

Screening and Selecting Raman Reporter Molecules

Five thiol molecules (2-MeOBT, 3-MeOBT, 4-MeOBT, 2-NT, and 4-NBT) were tested for potential Raman reporter use; their SERS spectra are shown in Figure 21. In order to compare the relative intensity of the Raman labels against each other, five micro-centrifuge tubes of ERLs were prepared. Each tube contained AuNPs modified with DTSSP mixed with one label molecule (mole ratio of 1:4), and goat anti-mouse IgG. After preparation, one drop of ERLs of each label was placed on a gold-coated glass slide and allowed to air dry. SERS spectra were collected on each spot. Four labels, 2-MeOBT, 4-MeOBT, 2-NT, and 4-NBT, provided distinct spectra, whereas no significant SERS signal was measured from 3-MeOBT. 4-MeOBT, 2-NT, and 4-NBT provided the unique bands, and therefore were selected to serve as Raman labels for a triplex assay. It is worth noticing that this experiment was used to qualitatively examine the distinctions in spectra of the label molecules; relative intensity was not taken into account. The three molecules can be differentiated based on the distinct signature peaks at 1378 cm^{-1} for 2-NT (ring stretching), 1336 cm^{-1} for 4-NBT (vibration of NO_2), and 1076 cm^{-1} for 4-MeOBT (vibration of S-C aromatic).

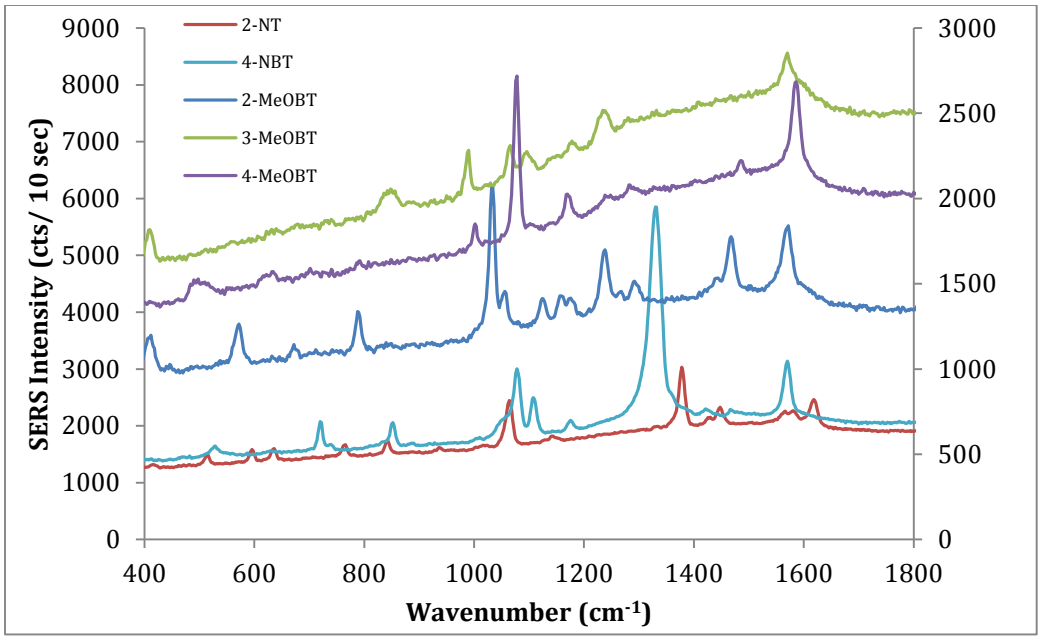

Figure 21. SERS spectra of the five Raman reporter molecules collected on the gold-coated glass slide. The intensities are not drawn to scale. The reporters with their signature peaks are 2-NT (red, 1378 cm^{-1}), 4-NBT (light blue, 1336 cm^{-1}), 2-MeOBT (dark blue, 1032 cm^{-1}), 3-MeOBT (green, 990 cm^{-1}), and 4-MeOBT (purple, 1076 cm^{-1}). The spectra of 4-NBT and 2-NT are drawn to the vertical axis on the left and those of 2-MeOBT, 3-MeOBT, and 4-MeOBT are drawn to the right axis.

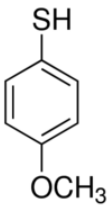

4-MeOBT

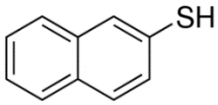

2-NT

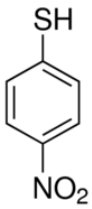

4-NBT

Figure 22. Chemical structures of 4-MeOBT, 2-NT, and 4-NBT

Customizing ERL Intensity

For multiplexed detection, having comparable intensities for all labels is also another feature we need to optimize. The significantly higher intensity of one Raman molecule may dominate the overall spectrum of the mixture and cause difficulty in signal identification and quantification. Wang *et al.* 2009 [26] showed that the scattering intensity of the Raman labels can be tuned by varying the ratio of linker (DTSSP) to reporter in the thiol mixture (the total concentration of thiols was kept constant at 15 nmol). ERLs were prepared by adding a mixed monolayer of DTSSP and a Raman reporter molecule to the AuNPs. Anti-mouse IgG was added to the modified AuNP. After assembly, ERLs were mixed with mouse IgG at the concentration of 5 μg/mL. The antigen-induced ERL aggregates were filtered through 200 nm pore membranes and allowed to dehydrate prior to SERS analysis. The dependence of SERS intensity on the mole fraction of 4-MeOBT was demonstrated via Figure 23. The intensity undergoes a steep increase when the mole fraction of 4-MeOBT is below 0.4 and starts to plateau when it reaches higher than 0.4 (as the label adsorption approaches surface saturation). Similar behavior was also observed with 4-NBT and 2-NT (data not shown).

Relating to the coating process, one could argue that the amount of DTSSP controls antibody coverage on the AuNP. In the mixture of the two thiols, as the amount of the label increased, the amount of DTSSP decreased. That might lead to less antibody adsorbed to AuNPs and affect the aggregation level as a result. Regarding this concern, Wang *et al* 2009 found that the number of antibodies coating the nanoparticles remains constant regardless of high or low concentration of DTSSP. Antibodies have much larger size relative to DTSSP and Raman labels; thus, one antibody molecule covers several

thiol molecules, only one of which needs to be DTSSP for linkage of the antibody. The binding of antibody and antigen therefore should be relatively similar over the range of the reporter/DTSSP ratios tested. It was indicated on the response curve that the mole fractions of 4-MeOBT, which were smaller than 0.4, resulted in less fluctuation in signal (smaller error bars). In addition, taking into account the relative intensities of the three labels, the optimal mole fraction for 4-MeOBT is 0.2 or 1:5 (i.e. one part of 4-MeOBT per four parts of DTSSP in the total 15 nmol thiol mixture), that for 4-NBT is 1:9, and that for 2-NT is 1:3.

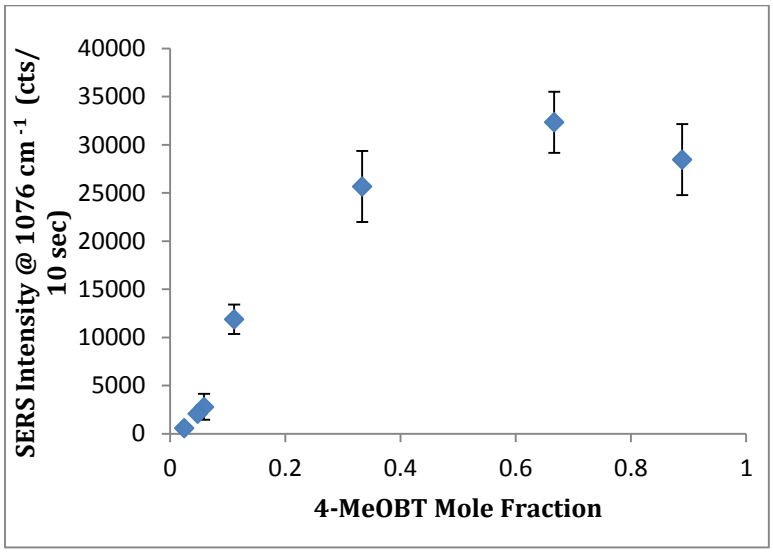

Figure 23. SERS intensity of ERLs as a function of the mole fraction of a Raman reporter molecules (4-MeOBT) in the thiol mixture with DTSSP to coat AuNPs. Each data point is the average of 2 independent experiments with standard deviations presented by error bars.

Analytical Performance of Singleplexed Assays

The specificity of anti-rabbit IgG modified ERLs was evaluated against rabbit IgG as on-target antigen and human and mouse IgG as off-target antigens separately via three singleplexed assays. The ERLs were produced by modification of AuNPs with anti-rabbit IgG antibody and 4-MeOBT as Raman label. ERLs from the same batch were mixed with three serial dilutions (0.5-50,000 ng/mL) of rabbit IgG, mouse IgG, or human IgG to investigate the specificity of the anti-rabbit against the on/off-target antigens. ERLs were mixed with PBS to serve as a blank control. The reaction was allowed to occur for 90 min in a 96-well plate. The mixtures then were transferred to microcuvettes and the mean hydrodynamic diameter of the particles was measured via DLS (as previously mentioned, DLS was used to validate the SERS result). It is clearly presented in Figure 24 that anti-rabbit antibody is specific to rabbit IgG but not mouse IgG and human IgG. The shape of the response curve of anti-rabbit versus rabbit IgG is similar to results previously reported in chapter II of this thesis and literature [10d, 53]; whereas, there was no significant change in the mean diameter of the ERLs after mixing with mouse IgG and human IgG. The mixtures of ERLs and specimen were passed through the 200 nm PCTE membranes placed in the microfiltration apparatus. After filtration the membrane filters were allowed to air dry prior to SERS analysis. This experiment was a replication of the similar experiment done with anti-mouse IgG and mouse IgG model in Lopez *et al.* 2015 [53], but replacing the home-built blotting apparatus with the microfiltration apparatus. The filtration occurred via vacuum suction instead of capillary action. This is one of the attempts to better concentrate aggregated nanoparticles (from 4.5 mm down to 3 mm for the spot size on the PCTE membrane) and to obtain more uniform distribution

of aggregates on the membrane surface to reduce the variation of SERS signal. The intensity of the peak at 1076 cm^{-1} (the strong vibration of S-C aromatic in 4-MeOBT molecule) was used to detect the formation of particle aggregates. Figure 25 indicates the SERS signal intensity obtained with off-target antigens was significantly lower than the one with on-target antigen at the antigen concentration of 500 ng/mL. Therefore, the selectivity of the assay was verified by both DLS and SERS analysis.

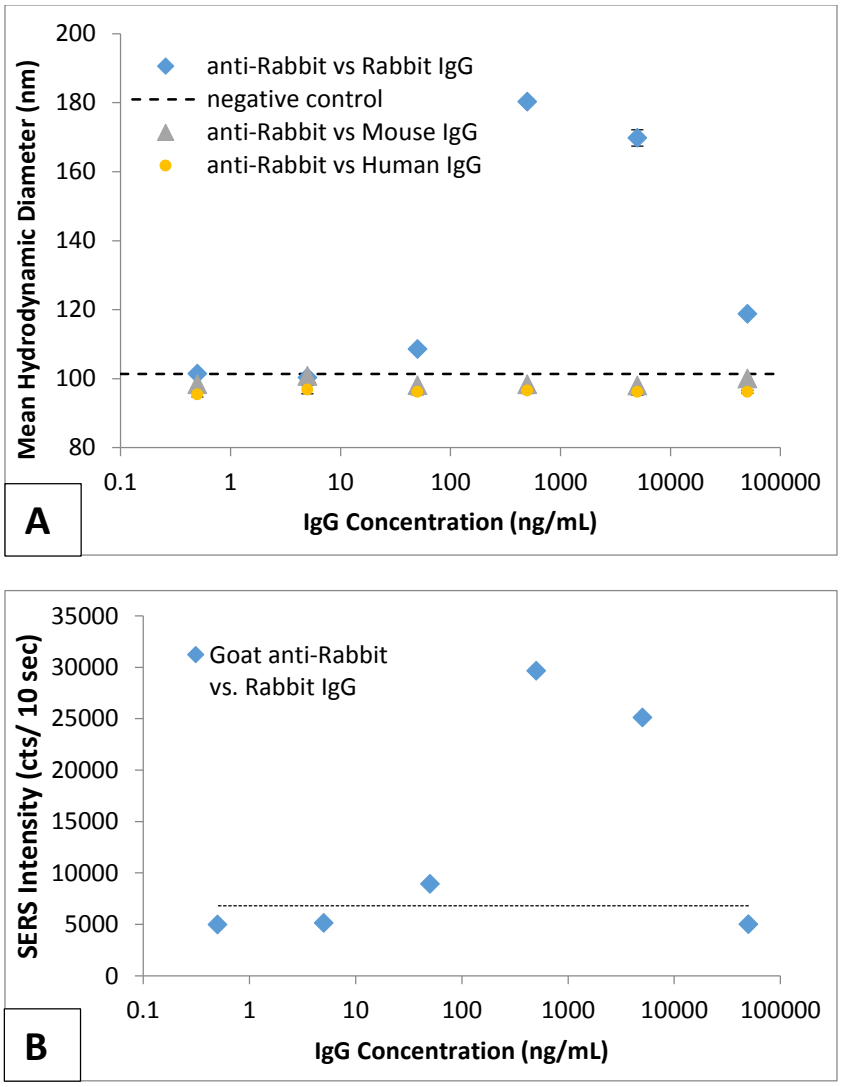

Figure 24. (A) Aggregation of ERLs as a function of rabbit IgG concentration (duplicated) versus anti-rabbit (blue diamond), anti-mouse (green triangle), and anti-human (purple circle) measured as an increase in hydrodynamic diameter via DLS. The dash line represents the negative control for the response curve of goat anti-rabbit ERLs vs rabbit IgG. (B) Goat anti-rabbit ERLs versus anti-rabbit calibration curve constructed using SERS data. The dash line represents the negative control.

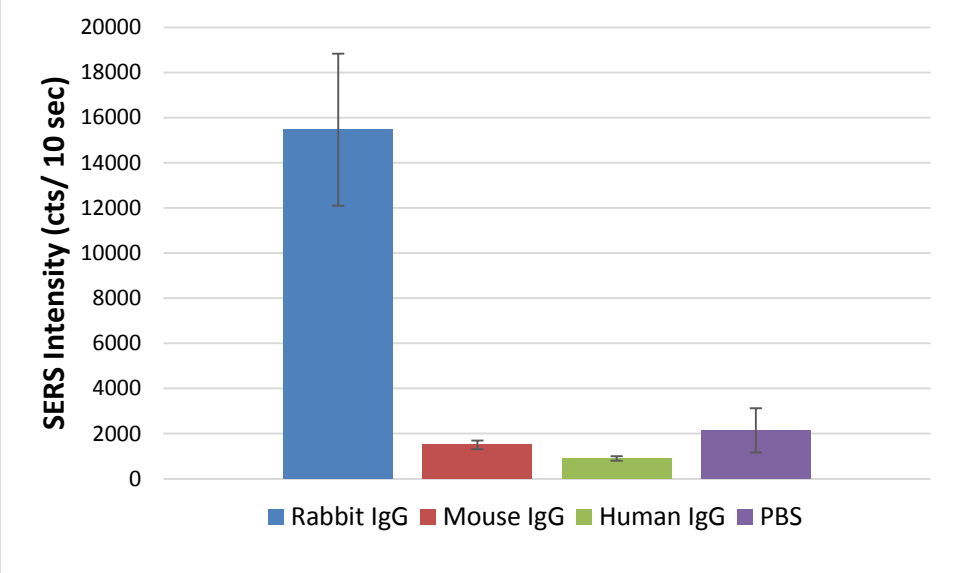

Figure 25. SERS intensity obtained from aggregated ERLs induced from mixing goat anti-rabbit ERLs with rabbit IgG, mouse IgG, and human IgG separately at the antigen concentration of 500 ng/mL and 0 ng/mL (or PBS). The experiment was done in duplicate.

Noticeably, the SERS signal collected from the negative control was quite significant; the detection limit of the assay via SERS, therefore, was highly affected. It is possible that some free ERLs were caught on the membrane surface during filtration due to non-specific binding or the use of not sufficiently large rinsing volume of buffer. Further investigation for filtration process needs to take place to eliminate undesired signal from negative controls and improve the sensitivity of the method.

CHAPTER IV

CONCLUSION AND FUTURE WORK

Research Summary

The preceding results lead to several remarks made via this research investigation. The focus of this work is to develop a multiplexed POC detection method for influenza A virus in a sensitive and timely manner. The first part of the thesis focuses on employing antibody-conjugated gold nanoparticles and dynamic light scattering for the study of conjugation assembly and monoclonal antibody screening. Namely, influenza-specific antibodies were attached to the surface of AuNPs, and aggregation was mediated by introduction of the target virus to the nanoparticle solution. A fundamental concern of the work was to ensure aggregates only formed in the presence of the virus not due to the instability of the particles; therefore, optimal conditions for maintaining the stability of the AuNPs coated with anti-influenza monoclonal antibodies, specifically for IgG1 and IgG2a isotypes, were investigated by varying pH, conjugation chemistry, and blocking reagents. Furthermore, DLS was exploited to screen the binding specificity of the anti-influenza antibodies to different strains of the virus, namely Influenza A/Puerto Rico/8/34 (H1N1) and A/New Caledonia/20/99 (H1N1). The extent of aggregation formed by mixing the mAb-AuNPs with the virus was measured to verify the specific interaction and binding affinity between the antibodies and virus. In addition, the DLS data were in good agreement with the results conducted with a well-established virus detection method, ELISA. Noticeably, DLS assay required 30 min to perform the same work that

took approximately 24 hours if using ELISA. This method offers a straight-forward protocol, high accuracy, low cost, and short assay time for monoclonal antibody screening. The insights obtained from the first part of the thesis have great contribution to better understand determining factors for the conjugation of monoclonal antibodies onto gold nanoparticles and the antibodies' binding characteristics to a specific antigen. It is also crucial to POC detection platform development because the selection of the most appropriate antibody for each individual antigen/pathogen is vital for the assay performance, especially selectivity.

The second part of the thesis demonstrated efforts devoted to develop an IA configuration coupled with SERS analysis for multiplexing. It is worth mentioning that viruses were not used in the development of the detection platform but human, rabbit, and mouse IgG were employed as model antigens instead since the research group recognizes more benefits can be gained when using the model of small antigens. First, IgG molecules are indeed proteins; thus, the method of detection developed for IgG molecules can also easily translated into the application of quantifying protein biomarkers. Second, in order to elevate the sensitivity of the method, the intact virus particle can be sliced open to free HA protein molecules from the viral membrane using some lysis buffer (potential future work). Then, 500 copies of HA from every virus particle are released into solution and become individual small targets in suspension. AuNP probes or ERLs have more possibility to form interaction with the antigen and induce aggregation. The detection of virus particles actually returns to the detection of small target indeed. This study has continued the work established to develop a SERS-based platform for singleplexed detection in Lopez *et al.* 2015. In that paper, polyclonal anti-mouse IgG

antibody and a Raman active label were directly immobilized on the AuNPs to produce ERLs. The ERLs after assembly were mixed with the sample containing mouse IgG antigen to induce aggregation. The ERL aggregate suspension was concentrated on a membrane and allowed to dehydrate prior to SERS analysis. The dependence of the analytical features of the assay on the membrane pore diameter and AuNP size was systematically investigated, and membranes of 200 nm pore diameter and 80 nm AuNPs were determined to provide maximal sensitivity. These optimizing elements were applied to the updated design of the platform studied in the second part of this thesis. There were some alterations in the ERL synthesis and blotting process make this design more adaptable to multiplexing. Firstly, selected antibody molecules were covalently conjugated on AuNPs via a bifunctional cross-linker (DTSSP in particular). The assistance of a cross-linker is anticipated to minimize the possibility of antibody exchange between ERLs since more than one type of ERLs are present in the solution. In addition to the primary function of DTSSP as a cross-linker, it also serves as the determining factor to customize the intensity of Raman labels in accordance to each other. The response curves dictating the dependence of labels' intensity on the ratio of DTSSP/Raman label were constructed to select the ratios such that no label has SERS intensity dominance and completely overwhelm the rest. The selected mole fractions were 1:9, 1:5, and 1:3 for 4-NBT, 4-MeOBT, and 2-NT, respectively. Secondly, the home-built Teflon blotting tool used in Lopez *et al*. 2015 was replaced by a 48 well Bio-blot apparatus to better concentrate the aggregated particles in a smaller spot to obtain stronger and more repeatable signals. Multiple samples were able to be filtered simultaneously to save more time and labor. However, in the attempts to replicate the

experiment, variations of signal from time to time were relatively large. The source of errors is not clear and therefore under further investigation.

Outlook and Future Work

To date, lateral flow assays still remain as the mainstream POC diagnostic platform for influenza virus detection but having the deficiencies of sensitivity and multiplexing. Great efforts from the scientific community have been devoted to address limitations of lateral flow assays. The utilization of nanoparticles as substrates in SERS-based homogeneous immunoassays has proven to pave the way for more advancement in POC diagnostic development. SERS-based homogeneous immunoassays potentially become an alternative for LFAs. It has been demonstrated in a recent study by the Jiang group [54] the capability of SERS-based homogeneous IAs to simultaneously detect three proteins with high sensitivity (namely 0.5 pM). The findings obtained from their research study will be applied to the continuing work of the Driskell group. Their work mainly focused on the synthetic strategies for the extrinsic labels. Antibody fragments are utilized in place of whole antibody molecules. The interparticle gaps between aggregated particles are anticipated to significantly decrease and therefore strongly elevate the SERS enhancement. The half antibody fragments are produced by the reduction of the whole antibodies by a mild reducing reagent, TCEP (tris(2-carboxyethyl) phosphine). TCEP breaks apart disulfide bonds that hold together two halves of the Y-shaped antibody. The thiol groups after cleaving are available for the covalent attachment of the half fragment to the gold surface. This will lead to the elimination of using DTSSP as a cross-linker in the protocol since half antibody fragments can be covalently conjugated to AuNP via direct adsorption. This approach is promising to more properly orient the antigen

binding-site and subsequently enhance the interaction of the ERLs to antigen. Better control over binding site orientation also would improve the reproducibility of the SERS immunoassay.

The new strategy of assembling ERLs, if successful with the antibodies we have in our lab, can be applied to our design for multiplexed assays. ERLs can be prepared by decorating AuNPs with TCEP-reduced antibody fragment. Raman labels will be mixed with DTSSP at the selected ratios and then added to the particle suspension. Herein DTSSP will only serve as a controlling factor for relative intensity of the Raman labels not as a cross-linker. Furthermore, more effort will be paid to the design and optimization of filtration apparatus to obtain a setup that can be incorporated to SERS hand-held devices.

REFERENCES

1.(a) Molinari, N.-A. M.; Ortega-Sanchez, I. R.; Messonnier, M. L.; Thompson, W. W.; Wortley, P. M.; Weintraub, E.; Bridges, C. B., The Annual Impact of Seasonal Influenza in the US: Measuring Disease Burden and Costs. *Vaccine* **2007,** *25* (27), 5086-5096; (b) Gatherer, D., The 2009 H1N1 Influenza Outbreak in Its Historical Context. *Journal of Clinical Virology* **2009,** *45* (3), 174-178.

2.Schnitzler, S. U.; Schnitzler, P., An Update on Swine-Origin Influenza Virus A/H1N1: a Review. *Virus Genes* **2009,** *39* (3), 279-292.

3.Taylor, J.; McPhie, K.; Druce, J.; Birch, C.; Dwyer, D. E., Evaluation of Twenty Rapid Antigen Tests for the Detection of Human Influenza A H5N1, H3N2, H1N1, and B Viruses. *Journal of Medical Virology* **2009,** *81* (11), 1918-22.

4.World Health Organization (WHO) Geographic Spread of Influenza Activity. http://gamapserver.who.int/h1n1/qualitative_indicators/atlas.html?indicator=i0&date=Week%2029%20(19-Jul-2010%20:%2025-Jul-2010) (accessed Feb 15, 2015).

5.(a) Peiris, J. M.; Poon, L. L.; Guan, Y., Emergence of a Novel Swine-Origin Influenza A Virus (S-OIV) H1N1 Virus in Humans. *Journal of Clinical Virology* **2009,** *45* (3), 169-173; (b) Sadana, A., *Biosensors: Kinetics of Binding and Dissociation Using Fractals*. Elsevier: **2003**, 184-204.

6.(a) Neumann, G.; Noda, T.; Kawaoka, Y., Emergence and Pandemic Potential of Swine-Origin H1N1 Influenza Virus. *Nature* **2009,** *459* (7249), 931-939; (b) Samji, T.,

Influenza A: Understanding the Viral Life Cycle. *The Yale Journal of Biology and Medicine* **2009,** *82* (4), 153.

7.Center for Disease Control (CDC) Images of Influenza Virus. http://www.cdc.gov/flu/images.htm (accessed Feb 21, 2015).

8.(a) Russi-Cahill, J. C.; Mogdasy, M. C.; Somma-Moreira, R. E.; de Peluffo, M. H., Counterimmunoelectrophoresis with Influenza Antigens. I. Use of Avian Plague Virus to Detect Type-Specific Antibodies to Influenza A in Human Sera. *The Journal of Infectious Diseases* **1975,** *131* (1), 64-6; (b) Leland, D. S.; Ginocchio, C. C., Role of Cell Culture for Virus Detection in the Age of Technology. *Clinical Microbiology Reviews* **2007,** *20* (1), 49-78.

9.(a) Chiapponi, C.; Moreno, A.; Barbieri, I.; Merenda, M.; Foni, E., Multiplex RT-PCR Assay for Differentiating European Swine Influenza Virus Subtypes H1N1, H1N2 and H3N2. *Journal of Virological Methods* **2012,** *184* (1-2), 117-20; (b) de-Paris, F.; Beck, C.; Machado, A. B.; Paiva, R. M.; da Silva Menezes, D.; de Souza Nunes, L.; Kuchenbecker, R.; Barth, A. L., Optimization of One-Step Duplex Real-Time RT-PCR for Detection of Influenza and Respiratory Syncytial Virus in Nasopharyngeal Aspirates. *Journal of Virological Methods* **2012,** *186* (1-2), 189-92; (c) Nguyen, T. T.; Kwon, H. J.; Kim, I. H.; Hong, S. M.; Seong, W. J.; Jang, J. W.; Kim, J. H., Multiplex Nested RT-PCR for Detecting Avian Influenza Virus, Infectious Bronchitis Virus and Newcastle Disease Virus. *Journal of Virological Methods* **2013,** *188* (1-2), 41-6; (d) Zhan, L.; Bao, L.; Li, F.; Lv, Q.; Xu, L.; Qin, C., An Optimized Real-Time PCR to Avoid Species-/Tissue-Associated Inhibition for H5N1 Detection in Ferret and Monkey Tissues. *The Scientific World Journal* **2012,** *2012*, 907095.

10.(a) Al-Yousif, Y.; Anderson, J.; Chard-Bergstrom, C.; Kapil, S., Development, Evaluation, and Application of Lateral-Flow Immunoassay (Immunochromatography) for Detection of Rotavirus in Bovine Fecal Samples. *Clinical and Diagnostic Laboratory Immunology* **2002,** *9* (3), 723-725; (b) Bodle, J.; Verity, E. E.; Ong, C.; Vandenberg, K.; Shaw, R.; Barr, I. G.; Rockman, S., Development of an Enzyme-Linked Immunoassay for the Quantitation of Influenza Haemagglutinin: an Alternative Method to Single Radial Immunodiffusion. *Influenza and Other Respiratory Viruses* **2013,** *7* (2), 191-200; (c) Chen, Y. T.; Tsao, Z.; Chang, S. T.; Juang, R. H.; Wang, L. C.; Chang, C. M.; Wang, C. H., Development of an Antigen-Capture Enzyme-Linked Immunosorbent Assay Using Monoclonal Antibodies for Detecting H6 Avian Influenza Viruses. *Journal of Microbiology, Immunology, and Infection* **2012,** *45* (3), 243-7; (d) Driskell, J. D.; Jones, C. A.; Tompkins, S. M.; Tripp, R. A., One-Step Assay for Detecting Influenza Virus Using Dynamic Light Scattering and Gold Nanoparticles. *Analyst* **2011,** *136* (15), 3083-3090; (e) Driskell, J. D.; Uhlenkamp, J. M.; Lipert, R. J.; Porter, M. D., Surface-Enhanced Raman Scattering Immunoassays Using a Rotated Capture Substrate. *Analytical Chemistry* **2007,** *79* (11), 4141-4148; (f) Ohnishi, K.; Takahashi, Y.; Kono, N.; Nakajima, N.; Mizukoshi, F.; Misawa, S.; Yamamoto, T.; Mitsuki, Y. Y.; Fu, S.; Hirayama, N.; Ohshima, M.; Ato, M.; Kageyama, T.; Odagiri, T.; Tashiro, M.; Kobayashi, K.; Itamura, S.; Tsunetsugu-Yokota, Y., Newly Established Monoclonal Antibodies for Immunological Detection of H5N1 Influenza Virus. *Japanese Journal of Infectious Diseases* **2012,** *65* (1), 19-27.

11.(a) Voller, A.; Bidwell, D.; Bartlett, A., Enzyme Immunoassays in Diagnostic Medicine: Theory and Practice*. *Bulletin of the World Health Organization* **1976,** *53* (1),

55; (b) Chun, P., Colloidal Gold and Other Labels for Lateral Flow Immunoassays. In *Lateral Flow Immunoassay*, Springer: **2009**; pp 1-19.

12.Pei, X.; Zhang, B.; Tang, J.; Liu, B.; Lai, W.; Tang, D., Sandwich-Type Immunosensors and Immunoassays Exploiting Nanostructure Labels: A review. *Analytica Chimica Acta* **2013,** *758*, 1-18.

13.Janeway, C. A.; Travers, P.; Walport, M.; Shlomchik, M. J., *Immunobiology: the Immune System in Health and Disease*. Churchill Livingstone London, 5th ed. New York: Garland Science; **2001** Vol. 2. The Structure of a Typical Antibody Molecule. http://www.ncbi.nlm.nih.gov/books/NBK27144/. (accessed Feb 20, 2015)

14.Chatenoud, L., Polyclonal and Monoclonal Antibodies. In *Therapeutic Immunosuppression*, Springer: **2001**; pp 55-80.

15.(a) Kato, H.; Torigoe, T., Radioimmunoassay for Tumor Antigen of Human Cervical Squamous Cell Carcinoma. *Cancer* **1977,** *40* (4), 1621-1628; (b) Abraham, G. E., Radioimmunoassay of Steroids in Biological Materials. *Acta Endocrinologica* **1974,** *75* (Supplement 183).

16.O'sullivan, M.; Bridges, J.; Marks, V., Enzyme Immunoassay: a Review. *Annals of Clinical Biochemistry: An International Journal of Biochemistry in Medicine* **1979,** *16* (1-6), 221-239.

17.(a) Hinshaw, J. C.; Toner, J. L.; Reynolds, G. A., Fluorescent labels for immunoassay. Google Patents: 1987; (b) Diamandis, E. P., Immunoassays with Time-Resolved Fluorescence Spectroscopy: Principles and Applications. *Clinical Biochemistry* **1988,** *21* (2), 139-150.

18.(a) Seitz, W. R., Immunoassay Labels Based on Chemiluminescence and Bioluminescence. *Clinical Biochemistry* **1984,** *17* (2), 120-125; (b) Miao, W., Electrogenerated Chemiluminescence and its Biorelated Applications. *Chemical Reviews* **2008,** *108* (7), 2506-2553.

19.(a) Penn, M. A.; Drake, D. M.; Driskell, J. D., Accelerated Surface-Enhanced Raman Spectroscopy (SERS)-Based Immunoassay on a Gold-Plated Membrane. *Analytical Chemistry* **2013,** *85* (18), 8609-17; (b) Medley, C. D.; Bamrungsap, S.; Tan, W.; Smith, J. E., Aptamer-Conjugated Nanoparticles for Cancer Cell Detection. *Analytical Chemistry* **2011,** *83* (3), 727-734; (c) James, A. E.; Driskell, J. D., Monitoring Gold Nanoparticle Conjugation and Analysis of Biomolecular Binding with Nanoparticle Tracking Analysis (NTA) and Dynamic Light Scattering (DLS). *Analyst* **2013,** *138* (4), 1212-1218.

20.(a) Akamizu, T.; Shinomiya, T.; Irako, T.; Fukunaga, M.; Nakai, Y.; Nakai, Y.; Kangawa, K., Separate Measurement of Plasma Levels of Acylated and Desacyl Ghrelin in Healthy Subjects Using a New Direct ELISA Assay. *The Journal of Clinical Endocrinology & Metabolism* **2005,** *90* (1), 6-9; (b) Beier, J. C.; Perkins, P. V.; Wirtz, R. A.; Koros, J.; Diggs, D.; Gargan, T. P.; Koech, D. K., Bloodmeal Identification by Direct Enzyme-Linked Immunosorbent Assay (ELISA), Tested on Anopheles (Diptera: Culicidae) in Kenya. *Journal of Medical Entomology* **1988,** *25* (1), 9-16.

21.Wild, D., *The Immunoassay Handbook*. Gulf Professional Publishing: 2005.

22.Paek, S.-H.; Lee, S.-H.; Cho, J.-H.; Kim, Y.-S., Development of Rapid One-Step Immunochromatographic Assay. *Methods* **2000,** *22* (1), 53-60.

23.O'Farrell, B., Evolution in Lateral Flow–Based Immunoassay Systems. In *Lateral Flow Immunoassay*, Springer: **2009**; pp 1-33.

24.(a) Taylor, J.; McPhie, K.; Druce, J.; Birch, C.; Dwyer, D. E., Evaluation of Twenty Rapid Antigen Tests for the Detection of Human Influenza A H5N1, H3N2, H1N1, and B Viruses. *Journal of Medical Virology* **2009,** *81* (11), 1918-1922; (b) Vasoo, S.; Stevens, J.; Singh, K., Rapid Antigen Tests for Diagnosis of Pandemic (Swine) Influenza A/H1N1. *Clinical Infectious Diseases* **2009,** *49* (7), 1090-1093.

25.Schmid, G., & Gade, L. H. Clusters and Colloids. From Theory to Applications. Angewandte Chemie-German Edition, **1995** *107*(4), 539-539.

26.Wang, G.; Park, H.-Y.; Lipert, R. J.; Porter, M. D., Mixed Monolayers on Gold Nanoparticle Labels for Multiplexed Surface-Enhanced Raman Scattering Based Immunoassays. *Analytical Chemistry* **2009,** *81* (23), 9643-9650.

27.(a) Aguilar, Z., *Nanomaterials for Medical Applications*. Newnes: **2012**; 127-138 (b) Guerrini, L.; Graham, D., Molecularly-Mediated Assemblies of Plasmonic Nanoparticles for Surface-Enhanced Raman Spectroscopy Applications. *Chemical Society Reviews* **2012,** *41* (21), 7085-7107.

28.(a) Ansari, S.; Freire, M.; Choi, M. G.; Tavari, A.; Almohaimeed, M.; Moshaverinia, A.; Zadeh, H. H., Effects of the Orientation of Anti-BMP2 Monoclonal Antibody Immobilized on Scaffold in Antibody-Mediated Osseous Regeneration. *Journal of Biomaterials Applications* **2015**, 0885328215594704; (b) Hermanson, G. T., *Bioconjugate Techniques*. Academic Press: **2013**, 582-586.

29.Berne, B. J.; Pecora, R., *Dynamic Light Scattering: with Applications to Chemistry, Biology, and Physics*. Courier Corporation: **2000**, 1-16.

30.Kim, H.-A.; Seo, J.-K.; Kim, T.; Lee, B.-T., Nanometrology and Its Perspectives in Environmental Research. *Environemtal Health Toxicology* **2014,** *29* (0), e2014016-0.

31.Jans, H.; Liu, X.; Austin, L.; Maes, G.; Huo, Q., Dynamic Light Scattering as a Powerful Tool for Gold Nanoparticle Bioconjugation and Biomolecular Binding Studies. *Analytical Chemistry* **2009,** *81* (22), 9425-9432.

32.Liu, X.; Huo, Q., A Washing-Free and Amplification-Free One-Step Homogeneous Assay for Protein Detection Using Gold Nanoparticle Probes and Dynamic Light Scattering. *Journal of Immunological Methods* **2009,** *349* (1), 38-44.

33.Liu, X.; Dai, Q.; Austin, L.; Coutts, J.; Knowles, G.; Zou, J.; Chen, H.; Huo, Q., A One-Step Homogeneous Immunoassay for Cancer Biomarker Detection Using Gold Nanoparticle Probes Coupled with Dynamic Light Scattering. *Journal of the American Chemical Society* **2008,** *130* (9), 2780-2782.

34.Fleischmann, M.; Hendra, P. J.; McQuillan, A., Raman Spectra of Pyridine Adsorbed at a Silver Electrode. *Chemical Physics Letters* **1974,** *26* (2), 163-166.

35.(a) Talley, C. E.; Jackson, J. B.; Oubre, C.; Grady, N. K.; Hollars, C. W.; Lane, S. M.; Huser, T. R.; Nordlander, P.; Halas, N. J., Surface-Enhanced Raman Scattering from Individual Au Nanoparticles and Nanoparticle Dimer Substrates. *Nano Letters* **2005,** *5* (8), 1569-1574; (b) Willets, K. A.; Van Duyne, R. P., Localized Surface Plasmon Resonance Spectroscopy and Sensing. *Annual Review of Physycal Chemistry* **2007,** *58*, 267-297.

36.(a) Tripp, R. A.; Dluhy, R. A.; Zhao, Y., Novel Nanostructures for SERS Biosensing. *Nano Today* **2008,** *3* (3), 31-37; (b) Porter, M. D.; Lipert, R. J.; Siperko, L. M.; Wang, G.; Narayanan, R., SERS as a Bioassay Platform: Fundamentals, Design, and Applications. *Chemical Society Reviews* **2008,** *37* (5), 1001-1011.

37.Lai, Y. H.; Koo, S.; Oh, S. H.; Driskell, E. A.; Driskell, J. D., Rapid Screening of Antibody–Antigen Binding Using Dynamic Light Scattering (DLS) and Gold Nanoparticles. *Analytical Methods* **2015**, *7*, 7249-7255

38.(a) Hoogenboom, H. R., Selecting and Screening Recombinant Antibody Libraries. *Nature Biotechnology* **2005,** *23* (9), 1105-1116; (b) Ylera, F.; Harth, S.; Waldherr, D.; Frisch, C.; Knappik, A., Off-rate screening for selection of high-affinity anti-drug antibodies. *Analytical Biochemistry* **2013,** *441* (2), 208-213.

39. Hall, S. S.; Daugherty, P. S., Quantitative Specificity-Based Display Library Screening Identifies Determinants of Antibody-Epitope Binding Specificity. *Protein Science* **2009,** *18* (9), 1926-1934.

40.Holt, L. J.; Büssow, K.; Walter, G.; Tomlinson, I. M., By-Passing Selection: Direct Screening for Antibody–Antigen Interactions Using Protein Arrays. *Nucleic Acids Research* **2000,** *28* (15), e72-e72.

41.(a) Dasary, S. S.; Senapati, D.; Singh, A. K.; Anjaneyulu, Y.; Yu, H.; Ray, P. C., Highly Sensitive and Selective Dynamic Light-Scattering Assay for TNT Detection Using p-ATP Attached Gold Nanoparticle. *ACS Applied Materials & Interfaces* **2010,** *2* (12), 3455-3460; (b) Xu, X.; Georganopoulou, D. G.; Hill, H. D.; Mirkin, C. A., Homogeneous Detection of Nucleic Acids Based Upon the Light Scattering Properties of Silver-Coated Nanoparticle Probes. *Analytical Chemistry* **2007,** *79* (17), 6650-6654.

42.Reed, L.; Muench, H., A Simple Method of Establishing 50% End Points. *American Journal of Hygyne* **1938,** *27*, 493-497.

43.Geoghegan, W. D.; Ambegaonkar, S.; Calvanico, N. J., Passive Gold Agglutination. An Alternative to Passive Hemagglutination. *Journal of Immunological Methods* **1980,** *34* (1), 11-21.

44.(a) Geoghegan, W. D., The Effect of Three Variables on Adsorption of Rabbit IgG to Colloidal Gold. *Journal of Histochemistry and Cytochemistry* **1988,** *36* (4), 401-407; (b) Geoghegan, W. D.; Ackerman, G. A., Adsorption of Horseradish-Peroxidase, Ovomucoid and Antiimmunoglobulin to Colloidal Gold for Indirect Detection of Concanavalin-a, Wheat-Germ Agglutinin and Goat Antihuman Immunoglobulin-g on Cell-Surfaces at Electron-Microscopic Level-New Method, Theory and Application. *Journal of Histochemistry and Cytochemistry* **1977,** *25* (11), 1187-1200.

45.Verkleij, A. J.; Leunissen, J. L., *Immuno-Gold-Labeling in Cell Biology*. CRC Press **1989**, 4-16.

46.Zhang, S.; Moustafa, Y.; Huo, Q., Different Interaction Modes of Biomolecules with Citrate-Capped Gold Nanoparticles. *ACS Applied Materials & Interfaces* **2014,** *6* (23), 21184-21192.

47.Driskell, J. D.; Kwarta, K. M.; Lipert, R. J.; Porter, M. D.; Neill, J. D.; Ridpath, J. F., Low-Level Detection of Viral Pathogens by a Surface-Enhanced Raman Scattering Based Immunoassay. *Analytical Chemistry* **2005,** *77* (19), 6147-6154.

48.(a) Ling, J.; Huang, C. Z.; Li, Y. F.; Zhang, L.; Chen, L. Q.; Zhen, S. J., Light-Scattering Signals from Nanoparticles in Biochemical Assay, Pharmaceutical Analysis and Biological Imaging. *TRAC Trends in Analytical Chemistry* **2009,** *28* (4), 447-453; (b) Yguerabide, J.; Yguerabide, E. E., Light-Scattering Submicroscopic Particles as Highly Fluorescent Analogs and Their Use as Tracer Labels in Clinical and Biological

Applications - II. Experimental Characterization. *Analytical Biochemistry* **1998,** *262* (2), 157-176.

49.Liedberg, B.; Ivarsson, B.; Hegg, P.-O.; Lundström, I., On the Adsorption of β-Lactoglobulin on Hydrophilic Gold Surfaces: Studies by Infrared Reflection-Absorption Spectroscopy and Ellipsometry. *Journal of Colloid and Interface Science* **1986,** *114* (2), 386-397.

50.Gufeng Wang, H.-Y. P., and Robert J. Lipert, Mixed Monolayers on Gold Nanoparticle labels for Multiplexed SERS. *Analytical Chemistry* **2009**, 81(23), 9643-9650.

51.Driskell, J. D.; Larrick, C. G.; Trunell, C., Effect of Hydration on Plasmonic Coupling of Bioconjugated Gold Nanoparticles Immobilized on a Gold Film Probed by Surface-Enhanced Raman Spectroscopy. *Langmuir* **2014,** *30* (22), 6309-6313.

52.Escamilla-Gómez, V.; Campuzano, S.; Pedrero, M.; Pingarrón, J. M., Gold Screen-Printed-Based Impedimetric Immunobiosensors for Direct and Sensitive Escherichia Coli Quantisation. *Biosensors and Bioelectronics* **2009,** *24* (11), 3365-3371.

53.Lopez, A.; Lovato, F.; Oh, S. H.; Lai, Y. H.; Filbrun, S.; Driskell, E. A.; Driskell, J. D., SERS Immunoassay Based on the Capture and Concentration of Antigen-Assembled Gold Nanoparticles. *Talanta* **2015**.

54.Wang, Y.; Tang, L.-J.; Jiang, J.-H., Surface-Enhanced Raman Spectroscopy-Based, Homogeneous, Multiplexed Immunoassay with Antibody-Fragments-Decorated Gold. *Analytical Chemistry* **2013,** *85* (19), 9213-9220.